and Machiedo, G. W.: Endotoxemia and bacteremia during hemorrhagic shock. *Ann. Surg.*, 207: 549–554 (1988).
27) Deith, E. A., Ma, W. J., Ma, L., Berg, R. and Specian, R. D.: Endotoxin-induced bacterial translocation: a study of mechanisms. *Surgery*, 106: 292–300 (1989).
28) Mori, T., Yamamoto, H., Tabata, T., Shimizu, T., Endo, Y., Hanasawa, K., Fujimiya, M. and Tani, T.: A free radical scavenger, edaravone (MCI-186), diminishes intestinal neutrophil lipid peroxidation and bacterial translocation in a rat hemorrhagic shock model. *Crit. Care Med.*, 33: 1064–1069 (2005).
29) Messingham, K. A., Faunce, D. E. and Kovacs, E. J.: Alcohol, injury, and cellular immunity. *Alcohol*, 28: 137–149 (2002).
30) Mathurin, P., Deng, Q. G., Keshavarzian, A., Choudhary, S., Holmes, E. W. and Tsukamoto, H.: Exacerbation of alcoholic liver by enteral endotoxin in rat. *Hepatology*, 32: 1008–1017 (2000).
31) Tamai, H., Kato, S., Horie, Y., Ohki, E., Yokoyama, H. and Ishii, H.: Effect of acute ethanol administration on the intestinal absorption of endotoxin in rat. *Alcohol. Clin. Exp. Res.*, 24: 390–394 (2000).
32) Jarvelainen, H. A., Fang, C., Ingelmann-Sundberg, M. and Lindros, K. O.: Effect of chronic coadministration of endotoxin and ethanol on rat liver pathology and pro-inflammatory and anti-inflammatory cytokines. *Hepatology*, 29: 1503–1510 (1999).
33) Morita, T., Naito, H., Ito, Y. and Nakajima, T.: Hypothesis of seven balances: molecular mechanisms behind alcoholic liver diseases and association with PPARα. *J. Occup. Health*, 51: 391–403 (2009).
34) Nanji, A. A., Khettry, U., Sadrzadeh, S. M. and Yamanaka, T.: Severity of liver injury in experimental alcoholic liver disease. Correlation with plasma endotoxin, prostaglandin E_2, leukotriene B_4, and thromboxane B_2. *Am. J. Pathol.*, 142: 367–373 (1993).
35) Thurman, R. G.: Mechanisms of hepatic toxicity II. Alcoholic liver injury involves activation of Kupffer cells by endotoxin. *Am. J. Physiol.*, 275: G605–G611 (1998).
36) Yin, M., Wheeler, M. D., Kono, H., Bradford, B. U., Gallucci, R. M., Luster, M. I. and Thurman, R. G.: Essential role of tumor necrosis factor alpha in alcohol-induced liver injury in mice. *Gastroenterology*, 117: 942–952 (1999).
37) Vidali, M., Stewart, S. F. and Albano, E.: Interplay between oxidative stress and immunity in the progression of alcohol-mediated liver injury. *Trends Mol. Med.*, 14: 63–71 (2008).
38) Takeda, K. and Akira, S.: TLR signaling pathways. *Semin. Immunol.*, 16: 3–9 (2004).
39) Szabo, G., Dolganiuc, A. and Mandrekar, P.: Pattern recognition receptors: a contemporary view on liver diseases. *Hepatology*, 44: 287–298 (2006).
40) Gutsmann, T., Müller, M., Carroll, S. F., MacKenzie, R. C., Wiese, A. and Seydel, U.: Dual role of lipopolysaccharide (LPS)-binding protein in neutralization of LPS and enhancement of LPS-induced activation of mononuclear cells. *Infect. Immun.*, 69: 6942–6950 (2001).
41) Uesugi, T., Froh, M., Arteel, G. E., Bradford, B. U., Wheeler, M. D., Gabele, E., Isayama, F. and Thurman, R. G.: Role of lipopolysaccharide-binding protein in early alcohol-induced liver injury in mice. *J. Immunol.*, 168: 2963–2969 (2002).
42) Yin, M., Bradford, B. U., Wheeler, M. D., Uesugi, T., Froh, M., Goyert, S. M. and Thurman, R. G.: Reduced early alcohol-induced liver injury in CD14-deficient mice. *J. Immunol.*, 166: 4737–4742 (2001).
43) Su, G. L., Klein, R. D., Aminlari, A., Zhang, H. Y., Steinstraeeser, L., Alarcon, W. H., Remick, D. G. and Wang, S. C.: Kupffer cell activation by lipopolysaccharide in rat: role for lipopolysaccharide binding protein and toll-like receptor 4. *Hepatology*, 31: 932–936 (2000).
44) Kono, H., Wheeler, M. D., Rusyn, I., Lin, M., Seabra, V., Rivera, C. A., Bradford, B. U., Forman, D. T. and Thurman, R. G.: Gender differences in early alcohol-induce liver injury: role of CD14, NF-κB, and TNF-α. *Am. J. Physiol. Gastrointest. Liver Physiol.*, 278: G652–G661 (2000).
45) Lukkari, T. A., Järveläinen, H. A., Oinonen, T., Kettunen, E. and Lindros, K. O.: Short-term ethanol exposure increases the expression of Kupffer cell CD14 receptor and lipopolysaccharide binding protein in rat liver. *Alcohol Alcohol.*, 34: 311–319 (1999).
46) Uesugi, T., Froh, M., Arteel, G. E., Bradford, B. U. and Thurman, R. G.: Toll-like receptor 4 is involved in the mechanism of early alcohol-induced liver injury in mice. *Hepatology*, 34: 101–108 (2001).
47) Tilg, H. and Diehl, A. M.: Cytokines in alcoholic and nonalcoholic steatohepatitis. *N. Engl. J. Med.*, 343: 1467–1476 (2000).
48) Yin, M., Gabele, E., Wheeler, M. D., Connor, H., Bradford, B. U., Dikalona, A., Rusyn, I., Mason, R. and Thurman, R. G.: Alcohol-induced free radicals in mice. Direct toxicants or signaling molecules? *Hepatology*, 34: 935–942 (2001).
49) Malhi, H., Gores, G. J. and Lemasters, J. J.: Apoptosis and necrosis in the liver: a tale of two deaths? *Hepatology*, 43: S31–S44 (2006).
50) Hsueh, W., Sun, X., Rjoja, L. N. and Gonzalez-Crussi, F.: The role of the complement system in shock and tissue injury induced by tumour necrosis factor and endotoxin. *Immunology*, 70: 309–314 (1990).
51) Leist, M., Gantner, F., Naumann, H., Bluethmann, H., Vogt, K., Brigelius-Flohe, R., Nicotera, P., Volk, H. D. and Wendel, A.: Tumor necrosis factor-induced apoptosis during the poisoning of mice with hepatotoxins. *Gastroenterology*, 112: 923–934 (1997).
52) Sakaguchi, S., Furusawa, S., Yokota, K., Sasaki, K., Takayanagi, M. and Takayanagi, Y.: The enhancing effect of tumour necrosis factor-α on oxidative stress in endotoxemia. *Pharmacol. Toxicol.*, 79: 259–265 (1996).
53) Sakaguchi, S., Furusawa, S., Yokota, K., Takayanagi, M. and Takayanagi, Y.: Modification of tumor necrosis factor-induced acute toxicity D-galactosamine challenge by polymyxin B, an anti-endotoxin. *Int. J. Immunopharmacol.*, 22: 935–942 (2000).
54) Sakaguchi, S. and Furusawa, S.: Oxidative stress and septic shock: metabolic aspects of oxygen-derived free radicals generated in the liver during endotoxemia. *FEMS Immunol. Med. Microbiol.*, 47: 167–177 (2006).
55) Ronis, M. J. J., Butura, A., Sampey, B. P., Prior, R. L., Korourian, S., Albano, E., Ingelman-Sundberg, M., Petersen, D. R. and Badger, T. M.: Effects of N-acetyl cysteine on ethanol-induced hepatotoxicity in rats fed via total enteral nutrition. *Free Radic. Biol. Med.*, 39: 619–630 (2005).
56) Vidali, M., Hietala, J., Occhino, G., Ivaldi, A., Sutti, S., Niemelä, O. and Albano, E.: Immune responses against oxidative stress-derived antigens are associated with increased circulating tumor necrosis factor-α in heavy drinkers. *Free Radic. Biol. Med.*, 45: 306–311 (2008).
57) Hill, D. B., Barve, S., Joshi-Barve, S. and McClain, C. J.: Increased monocyte nuclear factor-kappa B activation and tumor necrosis factor production in alcoholic hepatitis. *J. Lab. Clin. Med.*, 135: 387–395 (2000).
58) Pena, L. R., Hill, D. B. and McClain, C. J.: Treatment with glutathione precursor decreases cytokine activity. *JPEN J. Parenter. Enteral Nutr.*, 23: 1–6 (1999).
59) Yamashina, S., Takei, Y., Ikejima, K., Enomoto, N., Kitamura, T. and Sato, N.: Ethanol-induced sensitization to endotoxin in Kupffer cells is dependent upon oxidative stress. *Alcohol. Clin. Exp. Res.*, 29(12 Suppl.): 246S–250S (2005).
60) Lu, Y. and Cederbaum, A. I.: CYP2E1 and oxidative liver injury by alcohol. *Free Radic. Biol. Med.*, 44: 723–738 (2008).
61) Das, S. K. and Vasudevan, D. M.: Alcohol-induced oxidative stress.

Life Sci., 81: 177–187 (2007).
62) Salmela, K. S., Kessova, I. G., Tsyrlov, I. B. and Lieber, C. S.: Respective roles of human cytochrome P-4502E1, 1A2, and 3 in the hepatic microsomal ethanol oxidizing system. *Alcohol. Clin. Exp. Res.*, 22: 2125–2132 (1998).
63) Reinke, L. A.: Spin trapping evidence for alcohol-associated oxidative stress. *Free Radic. Biol. Med.*, 32: 953–957 (2002).
64) Bailey, S. M., Pietsch, E. C. and Cunningham, C. C.: Ethanol stimulates the production of reactive oxygen species at mitochondrial complexes I and III. *Free Radic. Biol. Med.*, 27: 891–900 (1999).
65) Fernandez-Checa, J. C., Kaplowitz, N., Garcia-Ruiz, C., Colell, A., Miranda, M., Mari, M., Ardite, E. and Morales, A.: GSH transport in mitochondria: defense against TNF-α induced oxidative stress and alcohol-induced defect. *Am. J. Physiol.*, 273: G7–G17 (1997).
66) Albano, E.: Alcohol, oxidative stress and free radical damage. *Proc. Nutr. Soc.*, 65: 278–290 (2006).
67) Mansouri, A., Demeilliers, C., Amsellem, S., Pessayre, D. and Fromenty, B.: Acute ethanol administration oxidatively damages and depletes mitochondrial DNA in mouse liver, brain, heart, and skeletal muscles: protective effects of antioxidants. *J. Pharmacol. Exp. Ther.*, 298: 737–743 (2001).
68) Zima, T. and Kalousova, M.: Oxidative stress and signal transduction pathways in alcoholic liver disease. *Alcohol. Clin. Exp. Res.*, 29: 110S–115S (2005).
69) Bradford, B. U., Kono, H., Isayama, F., Kosyk, O., Wheeler, M. D., Akiyama, T. E., Bleye, L., Krausz, K. W., Gonzalez, F. J., Koop, D. R. and Rusyn, I.: Cytochrome P450 CYP2E1, but not nicotinamide adenine dinucleotide phosphate oxidase, is required for ethanol-induced oxidative DNA damage in rodent liver. *Hepatology*, 41: 336–344 (2005).
70) Kono, H., Bradford, B. U., Yin, M., Sulik, K. K., Koop, D. R., Peters, J. M., Gonzalez, F. J., McDonald, T., Dikalova, A., Kadiska, M. B., Mason, R. P. and Thurman, R. G.: CYP2E1 is not involved in early alcohol-induced liver injury. *Am. J. Physiol.*, 277: G1259–G1267 (1999).
71) Vuppalanchi, R. and Chalasani, N.: Nonalcoholic fatty liver disease and nonalcoholic steatohepatitis: selected practical issues in their evaluation and management. *Hepatology*, 49: 306–317 (2009).
72) Bugianesi, E., McCullough, A. J. and Marchesini, G.: Insulin metabolic pathway to chronic liver disease. *Hepatology*, 42: 987–1000 (2005).
73) Tsochatzis, E. A., Manolakopoulos, S., Papatheodoridis, G. V. and Archimandritis, A. J.: Insulin resistance and metabolic syndrome in chronic liver diseases: old entities with new implication. *Scand. J. Gastroenterol.*, 44: 6–14 (2009).
74) Parkin, D. M.: Global cancer statistics in the year 2000. *Lancet Oncol.*, 2: 533–543 (2001).
75) Day, C. P. and James, O. F. W.: Steatohepatitis: a tale of two "hits". *Gastroenterology*, 114: 842–845 (1998).
76) Portincasa, P., Grattagliano, I., Palmieri, V. O. and Palasciano, G.: Nonalcoholic steatohepatitis: recent advances from experimental models to clinical management. *Clin. Biochem.*, 38: 203–217 (2005).
77) Diehl, A. M.: Lessons from animal models of NASH. *Hepatol. Res.*, 33: 138–144 (2005).
78) Gentile, C. L. and Pagliassotti, M. J.: The role of fatty acids in the development and progression of nonalcoholic fatty liver disease. *J. Nutr. Biochem.*, 19: 567–576 (2008).
79) Orellana, M., Rodrigo, R., Varela, N., Araya, J., Poniachik, J., Csendes, A., Smok, G. and Videla, L. A.: Relationship between *in vivo* chlorzoxazone hydroxylation, hepatic cytochrome P450 2E1 content and liver injury in obese non-alcoholic fatty liver disease patients. *Hepatol. Res.*, 34: 57–63 (2006).
80) Pessayre, D. and Fromenty, B.: NASH: a mitochondrial disease. *J. Hepatol.*, 42: 928–940 (2005).
81) Liu, H., Jones, B. E., Bradham, C. and Czaja, M. J.: Increased cytochrome P-450 2E1 expression sensitizes hepatocytes to c-Jun-mediated cell death from TNF-α. *Am. J. Physiol. Gastrointest. Liver Physiol.*, 282: G257–G266 (2002).
82) Kawaratani, H., Tsujimoto, T., Kitazawa, T., Kitada, M., Yoshiji, H., Uemura, M. and Fukui, H.: Innate immune reactivity of the liver in rats fed a choline-deficient L-amino-acid-defined diet. *World J. Gastroenterol.*, 14: 6655–6661 (2008).

Tumor Necrosis Factor-Alpha–Nuclear Factor-Kappa B-Signaling Enhances St2b2 Expression during 12-*O*-Tetradecanoylphorbol-13-acetate-Induced Epidermal Hyperplasia

Toshihiro MATSUDA,[a] Miki SHIMADA,*[,a,†] Akira SATO,[a] Takanori AKASE,[a] Kouichi YOSHINARI,[a] Kiyoshi NAGATA,[a,b] and Yasushi YAMAZOE[a,c]

[a] *Division of Drug Metabolism and Molecular Toxicology, Graduate School of Pharmaceutical Sciences, Tohoku University;* [c] *CRESCENDO, The Tohoku University 21st Century "Center of Excellence" Program; 6–3 Aramaki-Aoba, Aoba-ku, Sendai, Miyagi 980–8578, Japan: and* [b] *Department of Environmental and Health Science, Tohoku Pharmaceutical University; 4–4–1 Komatsusima, Aoba-ku, Sendai, Miyagi 981–8558, Japan.*
Received September 11, 2010; accepted November 5, 2010; published online November 12, 2010

The mouse cholesterol sulfotransferase St2b2 contributes to epidermal differentiation by biosynthesizing cholesterol sulfate (CS) from cholesterol in the epidermis. 12-*O*-Tetradecanoylphorbol-13-acetate (TPA) causes epidermal hyperplasia, an abnormal increase in epidermal cell numbers resulting from aberrant cell differentiation and an increase in St2b2 protein levels. The mechanisms underlying enhanced St2b2 expression and the pathophysiologic significance of the increased expression are unclear, however. To verify whether increased St2b2 levels are necessary for TPA-induced epidermal hyperplasia, the effects of St2b2-specific small hairpin RNA (St2b2-shRNA) on hyperplasia were examined in mice. St2b2-shRNA clearly suppressed TPA-induced epidermal hyperplasia and the expression of a marker of epidermal differentiation, involucrin (INV). Interestingly, treating mouse epidermal cells with tumor necrosis factor-alpha (TNFα) increased St2b2 expression. Furthermore, treatment with TNFα-siRNA or anti-TNF receptor antibodies reduced the TPA-induced enhancement of St2b2 expression. Treatment with BAY 11-7082, a specific inhibitor of nuclear factor-kappa B (NF-κB), diminished TPA-induced St2b2 expression. These results suggested that enhancement of St2b2 expression by TPA treatment occurs mainly through the TNFα–NF-κB inflammatory signaling pathway, which in turn leads to increased CS concentrations in epidermal cells and hyperplasia.

Key words cholesterol sulfate; epidermal differentiation; phorbol ester; nuclear factor-kappa B; sulfotransferase; tumor necrosis factor-alpha

Skin plays an essential role in protecting the body's internal environment against environmental insults. Keratinocyte differentiation, including expression of such cornified envelope proteins as involucrin (INV) and loricrin, is essential to maintain the structure and function of the epidermis. Disruption of the expression of these proteins causes epidermal dysplasia and dysfunction.[1,2)]

Treating skin with 12-*O*-tetradecanoylphorbol-13-acetate (TPA) causes epidermal hyperplasia through an abnormal increase in cornified envelope protein levels.[3)] TPA is thought to produce these effects by inducing protein kinase C (PKC) activation, calcium influx, and release of inflammatory cytokines, for example.[4—6)] The precise mediators of TPA signaling that cause epidermal hyperplasia, however, remain unclear.

Cholesterol sulfate (CS) is a chemical mediator that maintains epidermal homeostasis. Accumulation of CS—for instance, owning to a deficiency in the catabolic enzyme steroid sulfatase (SSase)—causes dyskeratosis.[7—9)] Levels of the CS biosynthetic enzyme cholesterol sulfotransferase (Ch-ST) are also associated with the extent of epidermal differentiation. In particular, St2b2, a member of the cytosolic sulfotransferase family, is the primary Ch-ST in mouse epidermis,[10)] where it plays a role in the expression of INV.[11)] Ch-ST activity increases together with cornified envelope protein levels after TPA treatment.[12,13)] Thus, St2b2 may be linked to TPA-induced epidermal hyperplasia.

Expressed beginning at early cornification, INV is involved in construction of the cornified envelope.[14,15)] Overexpression of INV distorts the structure of the epidermis.[1,16)] Furthermore, cells that express INV in response to various stimuli are selectively expelled from the basal layer composed of uncornified epidermal cells.[17)] Thus, INV expression levels can be used as a marker of the extent of epidermal differentiation.

Application of TPA on mouse skin causes an intense inflammatory response. The associated signaling is mediated by various cytokines and regulatory factors, such as tumor necrosis factor-alpha (TNFα) and interleukins, which are involved in epidermal differentiation and dyskeratosis.[18,19)] Indeed, TNFα levels increase when epidermis is exposed to TPA.[20,21)] TNFα binding to TNF receptor (TNFR) results in activation of a number of transcription factors, including nuclear factor-kappa B (NF-κB). Moreover, treating keratinocytes with anti-inflammatory drugs suppresses TPA-induced increases in Ch-ST activity,[13,22)] suggesting that TNFα–NF-κB signaling mediates TPA-induced enhancement of St2b2 expression.

The present study shows that TNFα–NF-κB signaling contributes to TPA-induced epidermal hyperplasia *via* increased St2b2 expression.

MATERIALS AND METHODS

Materials Cholesterol, CS, 3′-phosphoadenosine-5′-phos-

† Present address: *Department of Pharmaceutical Sciences, Tohoku University Hospital; 1–1 Seiryo-machi, Aoba-ku, Sendai, Miyagi 980–8574, Japan.*

* To whom correspondence should be addressed. e-mail: shimada@hosp.tohoku.ac.jp

phosulfate (PAPS), TPA, and alkaline phosphatase-conjugated goat anti-rabbit immunoglobulin G (IgG) were purchased from Sigma-Aldrich (St. Louis, MO, U.S.A.). [^{35}S]-PAPS and [^{14}C]-cholesterol was obtained from PerkinElmer Life and Analytical Sciences (Boston, MA, U.S.A.). PKCη pseudosubstrate inhibitor was purchased from Merck (Darmstadt, Germany). Recombinant mouse TNFα and mouse TNF enzyme-linked immunosorbent assay (ELISA) Kit 2 were purchased from Becton Dickinson Co. (San Diego, CA, U.S.A.). TNFα-small interfering RNA (siRNA), control-siRNA A, siRNA transfection medium, and siRNA transfection reagent were purchased from Santa Cruz Biotechnology (Santa Cruz, CA, U.S.A.). Anti-mouse TNFR hamster monoclonal antibodies (TNFR-Ab) were purchased from R&D Systems (Minneapolis, MN, U.S.A.). Hamster IgG (LEAF™ purified American hamster IgG isotype control Clone) was purchased from BioLegend (San Diego, CA, U.S.A.). BAY 11-7082 was purchased from BIOMOL Research Labs (Plymouth, PA, U.S.A.). The St2b2-specific small hairpin RNA (St2b2-shRNA)-expressing adenovirus AdSt2b2-shRNA was constructed previously.[11] All other chemicals used were of the highest grade available.

Animal Treatments Six-week-old female CD-1 mice (Charles River Japan, Atsugi, Japan) were housed in an air-conditioned room (22—23 °C) with a 12-h light period from 6 a.m. to 6 p.m. Food and water were available *ad libitum*. We used female mice in this study because epidermal St2b2 levels and cholesterol sulfation are slightly higher in females than in males.[10,11] Animal experiments were conducted in accordance with the guidelines of the Ministry of Education, Culture, Sports, Science and Technology of Japan. A dorsal area (2 cm^2) of each 6-week-old mouse was shaved using an electric shaver 24 h before the first treatment.

TPA treatment: TPA (16 nmol) dissolved in 200 μl of acetone (vehicle) was painted onto a shaved dorsal area of each mouse using a pipette. The skin was removed 40 h after treatment.

AdSt2b2-shRNA and TPA treatment: A previous report showed that a target gene could be introduced into epidermal cells by painting a mouse's skin with a suspension containing gene-encoding adenovirus.[11] Therefore, the shaved area of the mice was painted with a suspension containing 1.0×10^7 $TCID_{50}$ (50% titer culture infectious dose) of AdSt2b2-shRNA or control adenovirus (AdControl) 24 h before TPA treatment. TPA treatment was performed as described above.

Cell Treatments Neonatal mouse epidermal (NME) cells were prepared from newborn CD-1 mice, born to pregnant CD-1 mice (Charles River Japan, Atsugi, Japan), based on a previously reported method.[11] The cells were plated onto 100-mm dishes (treatment with AdSt2b2-shRNA and TPA) or 6-well plates (other experiments) at 3—4×10^5 cell/cm^2 and cultured in defined keratinocyte serum-free medium (SFM; 100-mm dishes, 10 ml; 6-well plates, 2 ml) (Invitrogen, Carlsbad, CA, U.S.A.). The first treatment was performed after 24 h of culture.

TPA treatment: NME cells were cultured in defined keratinocyte SFM containing 10 nM TPA or 0.1% (v/v) dimethyl sulfoxide (DMSO) (vehicle). Cells were harvested 0, 3, 6, 12, 24, or 40 h after TPA treatment.

AdSt2b2-shRNA and TPA treatment: NME cells were infected with AdSt2b2-shRNA (multiplicity of infection (MOI): 0, 1, 3, or 6) 24 h before TPA treatment. The total amount of adenovirus was adjusted to an MOI of 6 with AdControl. Cells were further cultivated in defined keratinocyte SFM containing 10 nM TPA or 0.1% (v/v) DMSO (vehicle) for 40 h.

PKC inhibitor and TPA treatment: The PKC inhibitor PKCη pseudosubstrate inhibitor was diluted to 0.5 or 1.5 mM with phosphate buffered saline (PBS) (vehicle). NME cells were incubated with 0.5 or 1.5 μM PKC inhibitor for 1 h. TPA (10 nM) treatment was performed as described above.

TNFα Treatment: Recombinant mouse TNFα was diluted to 10, 30, or 100 ng/ml with PBS containing 2 mg/ml BSA (vehicle). NME cells were cultivated in defined keratinocyte SFM containing TNFα (0, 10, 30, or 100 pg/ml) for 24 h.

AdSt2b2-shRNA and TNFα Treatment: NME cells were infected with AdSt2b2-shRNA or AdControl (MOI: 6) 24 h before TNFα treatment. Treatment with 30 pg/ml TNFα was carried out as described above.

TNFα-siRNA and TPA Treatment: Twenty-four hours before TPA treatment, NME cells were treated with TNFα-siRNA at 0, 15, 45, or 90 nM using siRNA transfection medium and siRNA transfection reagent. The concentration of siRNA was adjusted to 90 nM with Control-siRNA A. TPA (10 nM) treatment was performed as described above.

TNFR-Ab and TPA Treatment: NME cells were incubated with 0, 0.5, 2, or 8 μg/ml TNFR-Ab for 6 h. The total concentration of antibody was adjusted to 8 μg/ml with hamster IgG. TPA (10 nM) treatment was performed as described above.

NF-κB Inhibitor and TNFα Treatment: The NF-κB inhibitor BAY 11-7082 was dissolved to 1, 3, or 10 mM in DMSO (vehicle). NME cells were incubated with 0, 1, 3, or 10 μM BAY 11-7082 for 1 h. TNFα (30 pg/ml) treatment was performed as described above.

Preparation of Cytosolic, Microsomal, and Membrane Fractions Skin was removed and the dermis was excised from the skin by scraping with a surgical razor. The epidermis was homogenized in homogenizing buffer containing 75 mM potassium phosphate (pH 7.4), 75 mM KCl, and 1 mM dithiothreitol using a Polytron PT-10 homogenizer at 4 °C. The homogenate was filtered through gauze and centrifuged for 20 min at 4 °C and $9000\times g$. The resultant pellet was resuspended in homogenizing buffer and used as the membrane fraction. The supernatant (S-9) was further centrifuged for 60 min at 4 °C and $105000\times g$. The resultant supernatant was used as the cytosolic fraction, and the pellet was resuspended in homogenizing buffer and used as the microsomal fraction. NME cells were harvested and homogenized using homogenizing buffer. The homogenate was fractionated using the same method described for fractionation of epidermis. Protein concentrations were determined using the Bradford method.[23]

Immunoblotting Immunoblotting for St2b2 and INV was performed as described previously.[11] Cytosolic samples (20—40 μg of protein/lane) and membrane fractions (10—20 μg of protein/lane) were loaded.

Determination of Enzymatic Activities Cholesterol-sulfating activities were determined using a previously reported method.[11] The assay for CS desulfation was performed as described previously with some modifications.[24] SSase activity was determined based on desulfo-conjugation

Table 1. Primer Sequences for RT-PCRs

Gene		Sequence
St2b2	Sense	5'-TGTGGAGCTCGTCTGAGAAAAATGTT-3'
	Antisense	5'-TTGAAGGCGCTTATGATGGTCTCGC-3'
St2a4/9	Sense	5'-TGATGTCAGACTATAATTGGTTTGAAGGC-3'
	Antisense	5'-GGTTATGAGTCGTGGTCCTTCCTTATTG-3'
SSase	Sense	5'-GACGCTCGTCTACTTCACCTC-3'
	Antisense	5'-CTCCCAGTTGTTGCCCTTCC-3'
GAPDH	Sense	5'-TGCATCCTGCACCACCAACTG-3'
	Antisense	5'-GTCCACCACCCTGTTGCTGTAG-3'

of [^{14}C]-CS, which was prepared using [^{14}C]-cholesterol as a substrate, PAPS as a sulfate donor, and recombinant St2b2 protein, and purified using thin layer chromatography (TLC aluminum plate silica gel 60, Merck, Darmstadt, Germany). The desulfation assay was performed in 30 mM Tris–HCl buffer (pH 7.2) containing 0.25 M sucrose, 20 mM KCl, 5 mM $MgCl_2$, 1 mM dithiothreitol, 3 μM [^{14}C]-CS, and microsomal protein (100 μg) in a volume of 10 μl. The mixture was incubated at 37 °C for 12 h, and the reaction was terminated with 5 μl of acetonitrile. Ten-microliter aliquots of the reaction mixture were applied to a TLC plate. Metabolites on the chromatogram were developed using a solvent system of ethyl acetate/methanol/water (80 : 20 : 7.5 by vol). Radioactive spots were analyzed using a FLA-3000 image analyzer (Fujifilm Corporation, Tokyo, Japan).

Quantification of CS CS levels in epidermis and in NME cells were quantified as reported previously.[11)]

Isolation of Total RNA and Reverse Transcription-Polymerase Chain Reactions (RT-PCRs) Total RNA was prepared from epidermis tissue or NME cells using the acid guanidinium thiocyanate–phenol–chloroform method. mRNA levels were measured using RT-PCRs. The reaction conditions included 30 cycles of a three-phase PCR (denaturation at 95 °C for 15 s; annealing at 55 °C for 30 s; extension at 72 °C for 30 s). PCR products were analyzed on 2% (w/v) agarose gels containing ethidium bromide. The intensities of the stained bands were measured using NIH image software (version 1.59, Bethesda, MD, U.S.A.). The specific primers used for the PCRs are shown in Table 1.

Immunohistochemistry Dorsal skin was frozen in OCT Compound (Tissue-Tek, Sakura Finetechnical Co., Ltd., Tokyo, Japan). Specimens were sectioned using a cryostat and stained with methyl green-pyronin.

Detection of Intracellular and Extracellular TNFα Concentrations TNFα levels in the cells (S-9 fraction) and media were quantified using Mouse TNF ELISA Kit 2 in accordance with the manufacturer's instructions.

Statistical Analysis All data are shown as the means ± S.D. Statistical differences between groups were assessed by one-way ANOVA followed by Tukey's multiple comparison. Probability values less than 0.05 were considered statistically significant.

RESULTS

Effects of TPA Treatment on the Activities of Ch-ST and SSase in Mouse Skin To clarify the contributions of Ch-ST and SSase to the increased CS concentrations after TPA treatment, CS levels in skin, the specific activities of

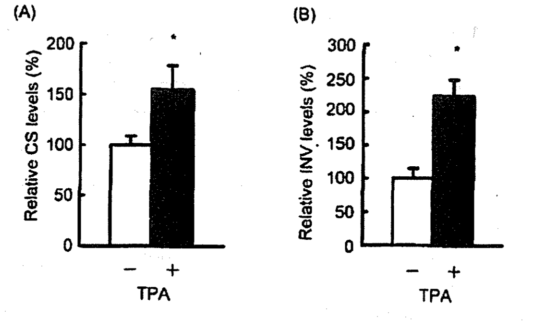

Fig. 1. Expression of CS and INV Protein in TPA-Treated Mouse Epidermis

TPA (16 nmol) dissolved in acetone (vehicle) was painted on shaved dorsal skin in mice. The skin was removed 40 h after treatment, and the dermis was excised. (A) The amount of CS in the epidermis was measured using thin layer chromatography. (B) INV levels in the membrane fraction from the epidermis were determined by immunoblotting. Expression levels are shown as ratios to levels observed in control TPA(−) epidermis. Data are shown as the means±S.D. ($n=3$). * $p<0.05$.

Table 2. Effects of TPA Treatment on Ch-ST and SSase Activities in Mouse Epidermis

Activity	Vehicle	TPA
Ch-ST (pmol/mg protein/min)	2.64±0.02	3.82±0.51*
SSase (pmol/mg protein/min)	0.69±0.11	0.78±0.08

Cytosolic protein and microsomal protein were examined from the epidermis used in Fig. 1. Methods used to determine the activities of Ch-ST in the cytosol and SSase in the microsomal fraction are provided in the Materials and Methods. Each value is shown as the mean±S.D. ($n=3$). * $p<0.05$.

Ch-ST and SSase, and St2b2, St2a4/9, and SSase mRNA levels were determined. Skin INV protein levels were used as a marker of epidermal differentiation. After TPA treatment, CS levels in mouse epidermis were 50% higher than those in control TPA(−) skin (Fig. 1A). TPA treatment also enhanced INV expression (120% increase; Fig. 1B) and skin Ch-ST activity (40% increase; Table 2). St2b2 mRNA and protein levels in skin increased by 120% and 50%, respectively (Fig. 2). Neither the activity nor mRNA levels of SSase changed significantly, however (Fig. 2, Table 2). In addition, mRNA encoding St2a4 or St2a9, which mediate cholesterol sulfation in mice, was not detected in normal mouse epidermal cells, as reported previously,[10)] or in TPA-treated skin (Fig. 2).

Effects of AdSt2b2-shRNA on TPA-Induced Epidermal Differentiation in NME Cells St2b2-shRNA was then administered to NME cells and the levels of CS and INV protein were examined (Fig. 3). St2b2 protein levels increased by 40% after TPA treatment in control AdSt2b2-shRNA(−) cells, whereas they MOI-dependently decreased in response to AdSt2b2-shRNA. St2b2 expression decreased to 80% of that observed in control TPA(−) cells (Fig. 3A). Consistent with this finding, CS levels also decreased to 60% of those observed in control cells following infection with AdSt2b2-shRNA (MOI, 6; Fig. 3B). A correlation was observed between the levels of CS and St2b2 protein (Fig. 3D). The TPA-mediated increase in INV expression levels was attenuated to 90% of levels detected in control cells following infection with AdSt2b2-shRNA (MOI, 6: Fig. 3C). A correlation was observed between expression levels of INV and St2b2 (Fig. 3E). SSase mRNA levels were not affected by infection with AdSt2b2-shRNA (data not shown).

Effects of a PKC Inhibitor on TPA-Induced Increases in St2b2 and INV Expression in NME Cells The effects of a PKC inhibitor on St2b2 and INV protein levels were then examined during TPA-induced epidermal differentiation in NME cells. After TPA treatment, St2b2 protein levels increased to 160% of those observed in control cells (PKC inhibitor(−) and TPA(−)); the PKC inhibitor (0.5 or 1.5 μM) did not significantly affect St2b2 levels (Fig. 4A). Expression levels of INV protein also increased to 160% of those observed in control cells after TPA treatment, whereas, in response to 1.5 μM PKC inhibitor, the level decreased to 70% of that detected in control cells (Fig. 4B).

Knocking Down St2b2 Gene Expression during TPA-Induced Epidermal Hyperplasia in Mouse Skin The effects of knocking down St2b2 gene expression were then examined during epidermal hyperplasia. As shown in Fig. 5, the thickness of the epidermis increased after TPA treatment, but not when AdSt2b2-shRNA was also introduced together with TPA. We also examined Ch-ST activity and expression

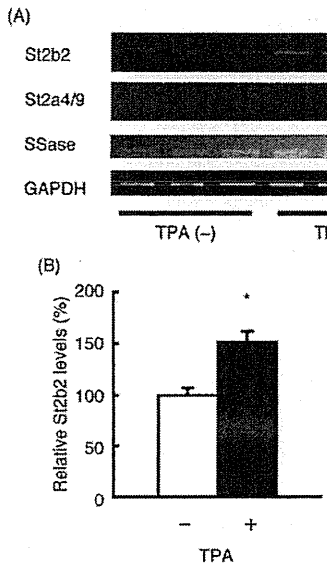

Fig. 2. Expression of St2b2, St2a4/9, and SSase mRNA and St2b2 Protein in Mouse Epidermis after Treatment with TPA

Total RNA and cytosolic protein were prepared from the epidermis used in Fig. 1. (A) mRNA levels were measured using RT-PCRs. (B) St2b2 protein levels in the cytosol were determined by immunoblotting. Expression levels are shown as ratios to those in control TPA(−) epidermis. Data are shown as the means±S.D. (n=3). * p<0.05.

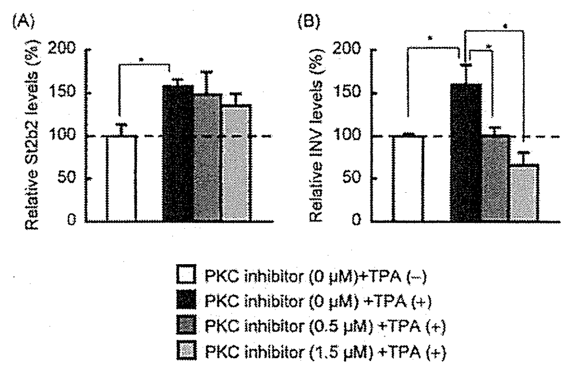

Fig. 4. Effects of PKC Inhibitor Treatment on St2b2 and INV Expression in NME Cells

NME cells (3×10^5 cells/cm^2) were incubated with PKCη pseudosubstrate (0.5 or 1.5 μM) for 1 h, and then cultivated with 10 nM TPA or 0.1% (v/v) DMSO (vehicle) for 24 h. Levels of St2b2 protein in the cytosol (A) and INV protein in the membrane fraction (B) were determined by immunoblotting. Expression levels are shown as ratios to those in control PKC inhibitor(−) and TPA(−) cells. Data are shown as means±S.D. (n=3). * p<0.05.

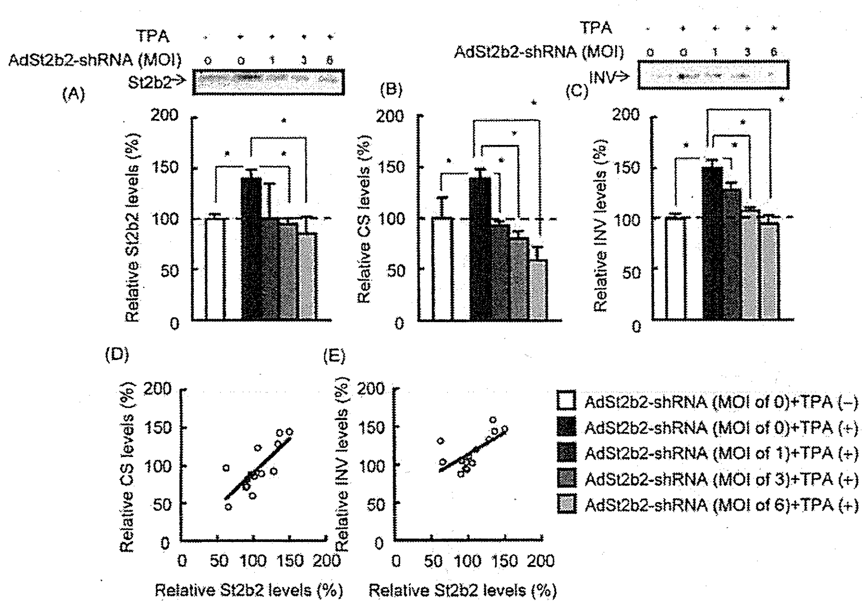

Fig. 3. Effects of AdSt2b2-shRNA Infection on TPA-Induced Epidermal Differentiation in NME Cells

NME cells (3×10^5 cells/cm^2) were infected with AdSt2b2-shRNA (MOI: 1, 3, or 6) 24 h before TPA treatment. The total amount of adenovirus was adjusted to an MOI of 6 using AdControl. Cells were then treated with 10 nM TPA or 0.1% (v/v) DMSO (vehicle), and harvested 40 h later. The cells were subjected to the following analyses. (A) Expression of St2b2. Example immunoblotting of St2b2 in the cytosol is shown above the graph. (B) CS levels were quantified using thin layer chromatography. (C) Expression of INV. Example immunoblotting of INV in the membrane fraction above the graph. (D) Correlation between St2b2 expression and CS levels. (E) Correlation between protein expression of St2b2 and INV. Expression levels are shown as ratios to those observed in control AdSt2b2-shRNA(−) and TPA(−) cells. Data are shown as the means±S.D. (n=3). * p<0.05.

of St2b2 and INV. St2b2 protein levels decreased to 60% of those in control skin following infection with AdSt2b2-shRNA (Fig. 6A). St2b2 proteins level increased by 30% after TPA treatment in control skin, but were not significantly affected by TPA treatment in AdSt2b2-shRNA–infected skin (Fig. 6A). Ch-ST activity also increased by 50% after TPA treatment in control skin, but not in AdSt2b2-shRNA–infected skin (Fig. 6B). INV protein levels increased by 40% after TPA treatment in control skin, but not in AdSt2b2-shRNA–infected skin (Fig. 6C).

Time-Dependent Changes in St2b2, INV, and TNFα Expression after TPA Treatment in NME Cells To explore the potential involvement of TNFα in TPA-induced enhancement of St2b2 and INV expression, time-dependent changes in the expression profiles of these proteins were examined after TPA treatment in NME cells. Significant increases in St2b2 expression were observed after 24 h (Fig. 7A). INV expression also increased after 24 h (Fig. 7B). Cellular levels of TNFα protein peaked within 3 h of TPA treatment (Fig. 7C), whereas extracellular levels reached a maximum at 24 h (Fig. 7D).

Effects of TNFα on St2b2 and INV Expression in NME Cells To examine the role of TNFα in TPA-induced enhancement of St2b2 expression, NME cells were treated with TNFα. St2b2 protein levels increased by up to 260% after TNFα treatment (Fig. 8A). INV protein levels also similarly increased (by a maximum of 210%; Fig. 8B). Maximum effects for both proteins were observed with 30 pg/ml TNFα.

Effects of Knocking Down St2b2 Expression on TNFα-Induced INV Expression in NME Cells AdSt2b2-shRNA was then used to examine the roles of St2b2 on enhanced INV expression in NME cells. St2b2 protein expression levels in TNFα-treated cells decreased from 410 to 130% of those observed in control cells after AdSt2b2-shRNA infection (Fig. 9A). AdSt2b2-shRNA infection also decreased INV protein expression in TNFα-treated cells from 330 to 130% of control levels (Fig. 9B).

Effects of Inhibiting TNFα Signaling on TPA-Induced Enhancement of St2b2 and INV Expression in NME Cells To verify that TNFα signaling mediates the TPA-induced enhancement of St2b2 and INV expression, TNFα-siRNA was introduced into NME cells. TNFα protein levels in the

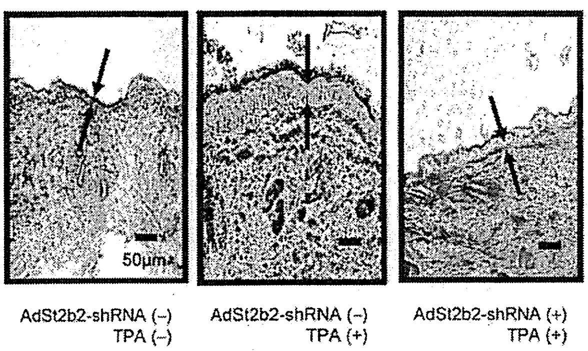

Fig. 5. Effects of AdSt2b2-shRNA on TPA-Induced Hyperplasia in Mouse Epidermis

Shaved skin was painted with a suspension containing 1.0×10^7 TCID$_{50}$ of AdSt2b2-shRNA or AdControl, and the mice were treated with TPA (16 nmol) or acetone (vehicle) 24 h after adenovirus infection. The skin was removed 40 h after TPA treatment. The thickness of the epidermis was determined using frozen sections stained with methyl green-pyronin. The epidermis is shown between the arrows. Scale bars represent 50 μm.

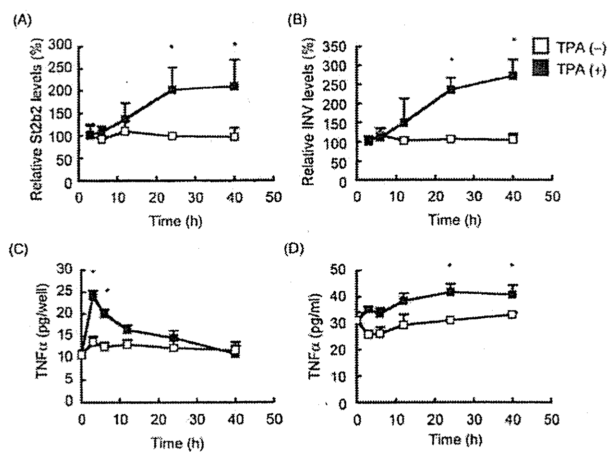

Fig. 7. Expression of TNFα, St2b2, and INV after TPA Treatment in NME Cells

NME cells (3×10^5 cells/cm^2) were cultured in medium containing 10 nM TPA or 0.1% (v/v) DMSO (vehicle), and harvested 0, 3, 6, 12, 24, or 40 h after TPA treatment. Levels of St2b2 protein in the cytosol (A) and INV protein in the membrane fraction (B) were determined by immunoblotting. The levels are shown as ratios to those detected at 3 h. TNFα levels in the S-9 fraction (C) and the medium (D) were determined using ELISAs. Data are shown as means$\pm$S.D. ($n=3$). $*p<0.05$ (St2b2 and INV, *vs.* vehicle-treated TPA(−) cells at 3 h; TNFα, *vs.* vehicle-treated TPA(−) cells at 0 h).

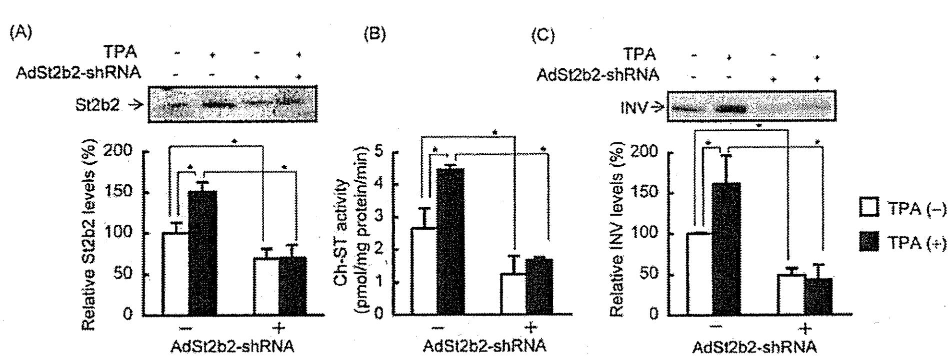

Fig. 6. Effects of Knocking Down St2b2 Gene Expression on TPA-Induced Epidermal Differentiation

Mice were treated with AdSt2b2-shRNA and TPA as described in the legend for Fig. 5. Levels of St2b2 protein in the cytosol (A) and INV protein in the membrane fraction (B) were determined by immunoblotting. Membranes immunoblotted for St2b2 and INV are shown above the graphs. The expression levels are shown as ratios to those in control AdSt2b2-shRNA(−) and TPA(−) epidermis. Ch-ST activity in the cytosol (C) was also assessed. Data are shown as means$\pm$S.D. ($n=3$). $*p<0.05$.

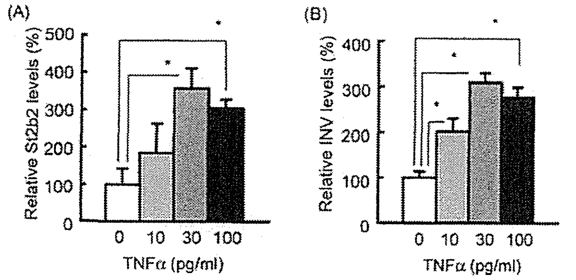

Fig. 8. Effects of TNFα Treatment on St2b2 and INV Expression in NME Cells

NME cells (3×10^5 cells/cm^2) were cultivated in medium containing TNFα (10, 30, or 100 pg/ml) or 2 μg/ml BSA-PBS (vehicle) for 24 h. Levels of St2b2 protein in the cytosol (A) and INV protein in the membrane fraction (B) were determined by immunoblotting. The expression levels are shown as ratios to those in control cells. Data are shown as means±S.D. ($n=3$). *$p<0.05$ *vs.* vehicle-treated TNFα(−) cells.

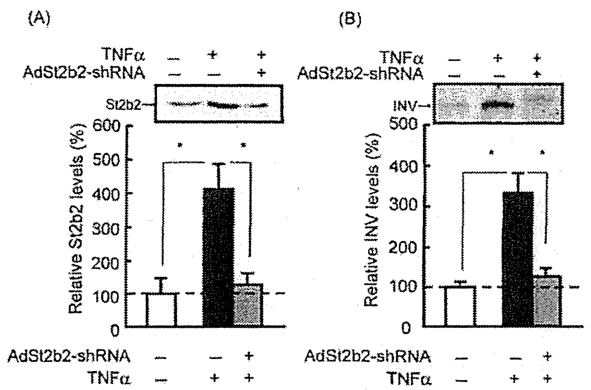

Fig. 9. Effects of Knocking Down St2b2 Expression on TNFα-Induced Enhancement of St2b2 and INV Expression in NME Cells

NME cells (3×10^5 cells/cm^2) were infected with AdSt2b2-shRNA (MOI: 6), and, 24 h later, the cells were treated with 30 pg/ml TNFα or 2 μg/ml BSA-PBS (vehicle) for 24 h. Levels of St2b2 protein in the cytosol (A) and INV protein in the membrane fraction (B) were determined by immunoblotting. Membranes immunoblotted for St2b2 and INV are shown above the graphs. Expression levels are shown as ratios to those in control AdSt2b2-shRNA(−) and TNFα(−) cells. Data are shown as means±S.D. ($n=3$). *$p<0.05$.

medium increased to 45 pg/ml after TPA treatment (control cells produced 21 pg/ml). On the other hand, TNFα protein levels did not increase after TPA treatment in the presence of TNFα-siRNA; TPA-treated cells that were also exposed to 90 nM TNFα-siRNA produced 22 pg/ml TNFα (Fig. 10A). St2b2 protein levels in TPA-treated cells (190% of levels detected in control cells) decreased to 100% of those observed in control cells after treatment with 90 nM TNFα-siRNA (Fig. 10B). TPA-induced enhancement of INV expression (150% of levels in control cells) also decreased to 100% of that in control cells after treatment (Fig. 10C).

To confirm further the involvement of TNFα in TPA-induced enhancement of St2b2 and INV expression, St2b2 and INV protein levels were examined in NME cells treated with TNFR-Ab and TPA. TNF-Ab (8 μg/ml) reduced TPA-induced enhancement of St2b2 expression (170% of that in control TNFR-Ab(−) and TPA(−) cells) to 70% of that observed in the control cells (Fig. 11A). The TPA-induced enhancement of INV expression (160% of that in control cells) was also reduced to 110% of that detected in control cells after treatment (Fig. 11B). No marked difference was observed in extracellular TNFα protein levels before and

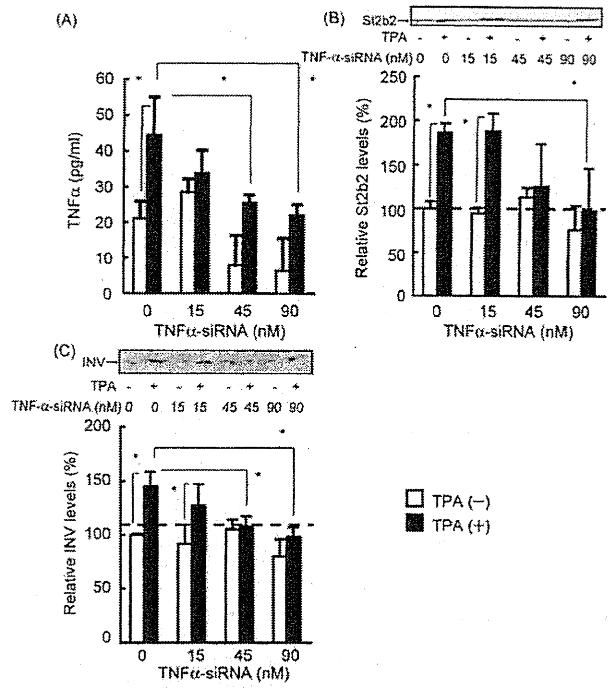

Fig. 10. Effects of Knocking Down TNFα Expression on TPA-Induced Enhancement of St2b2 and INV Expression in NME Cells

NME cells (3×10^5 cells/cm^2) were transfected with TNFα-siRNA (15, 45, or 90 nM). The total amount of siRNA was adjusted to 90 nM using Control-siRNA A. Twenty-four hours later, the cells were treated with 10 nM TPA or 0.1% (v/v) DMSO (vehicle) for 40 h. (A) TNFα protein levels in the medium were determined using an ELISA. Levels of St2b2 protein in the cytosol (B) and INV protein in the membrane fraction (C) were determined by immunoblotting. Expression levels are shown as ratios to those in control TNFα-siRNA(−) and TPA(−) cells. Data are shown as means±S.D. ($n=3$). *$p<0.05$.

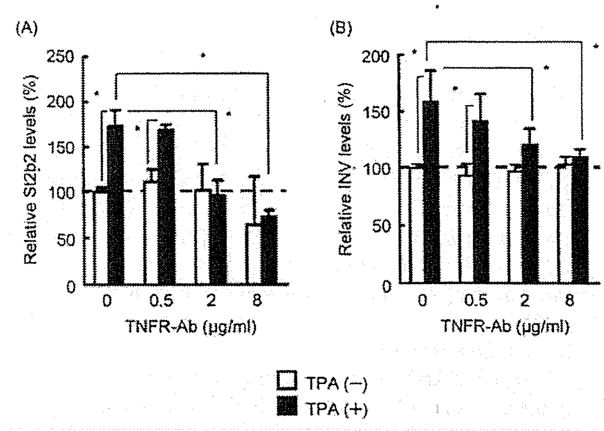

Fig. 11. Effects of TNFR Inhibition on TPA-Induced Enhancement of St2b2 and INV Expression in NME Cells

NME cells (3×10^5 cells/cm^2) were incubated with 0.5, 2, or 8 μg/ml TNFR-Ab for 6 h. The total amount of antibody was adjusted to 8 μg/ml with normal IgG. The cells were then cultivated in medium containing 10 nM TPA or 0.1% (v/v) DMSO (vehicle) for 40 h. St2b2 protein levels in the cytosol (A) and INV protein levels in the membrane fraction (B) were determined by immunoblotting. Expression levels are shown as ratios to those in control TNFR-Ab(−) and TPA(−) cells. Data are shown as means±S.D. ($n=3$). *$p<0.05$.

after treatment (data not shown).

Effects of NF-κB Inhibition on TNFα-Induced Enhancement of St2b2 and INV Expression in NME Cells NF-κB, which is activated through TNFα–TNFR signaling,

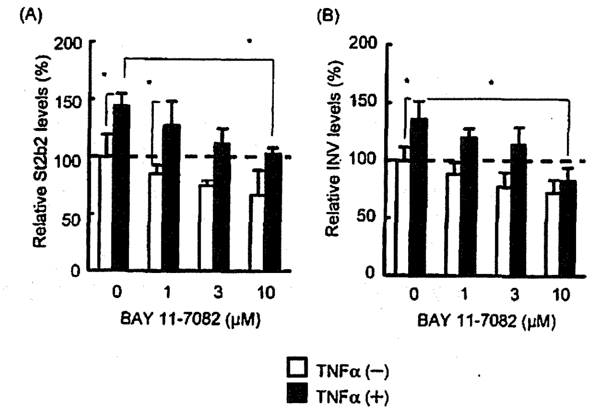

Fig. 12. Effects of NF-κB Inhibition on TNFα-Induced Enhancement of St2b2 and INV Expression in NME Cells

NME cells (3×10^5 cells/cm^2) were incubated with BAY 11-7082 (1, 3, or 10 μM) for 1 h, and then cultivated with 30 pg/ml TNFα or 2 μg/ml BSA-PBS (vehicle) for 24 h. Levels of St2b2 protein in the cytosol (A) and INV protein in the membrane fraction (B) were determined by immunoblotting. Expression levels are shown as ratios to those in the control BAY 11-7082(−) and TNFα(−) cells. Data are shown as the means±S.D. ($n=3$). * $p<0.05$.

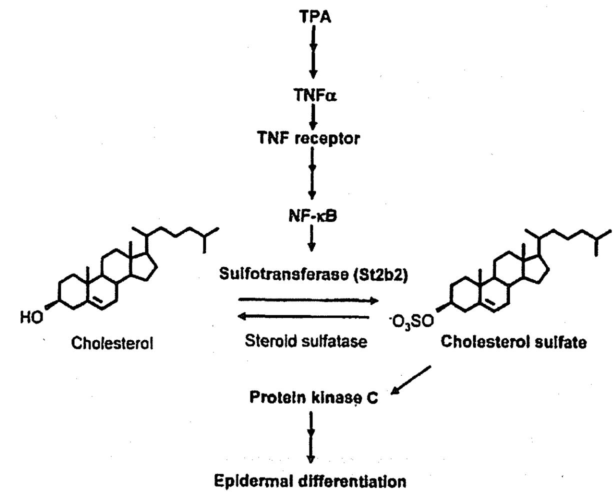

Fig. 13. A Putative Pathway for TPA-Induced Epidermal Differentiation through St2b2

plays a critical role in cell differentiation.[25] To examine NF-κB during TPA-induced enhancement of St2b2 and INV expression, an NF-κB inhibitor, BAY 11-7082, was administered to NME cells. BAY 11-7082 (10 μM) decreased TNFα-induced enhancement of St2b2 expression (140% of that in control BAY 11-7082(−) and TNFα(−) cells) to 100% of that in control cells (Fig. 12A). TNFα-induced enhancement of INV expression (140% of levels observed in control cells) decreased to 80% of levels in control cells after treatment (Fig. 12B).

DISCUSSION

CS is involved in epidermal differentiation and, at high concentrations, causes epidermal hyperplasia. Skin CS levels are believed to be maintained by both Ch-ST and SSase. In the present study, TPA-mediated CS accumulation in the epidermis occurred in parallel with increased Ch-ST activity, without changes in SSase activity (Table 2). Expression of St2b2 mRNA and protein in mouse skin increased after TPA treatment (Fig. 2). These results were consistent with the idea that TPA-mediated CS production mainly results from enhanced St2b2 expression.

To assess St2b2 functions during TPA-induced epidermal hyperplasia and differentiation, St2b2 gene expression was knocked down using shRNA in mice. TPA-induced epidermal hyperplasia was clearly blocked by St2b2-shRNA (Fig. 5). Decreases in INV and St2b2 expression were also observed in epidermis tissue infected with AdSt2b2-shRNA (Fig. 6). These results suggested that an increase in St2b2 levels is a prerequisite for TPA-induced epidermal hyperplasia.

PKC activation is involved in the differentiation of many cell lines, including epidermal cells, and is a key process during TPA-induced epidermal differentiation.[26—28] TPA was reported to activate PKC *via* direct binding[29]; this study suggested that direct binding triggers TPA-induced epidermal differentiation, but the mechanism for PKC activation during TPA-induced epidermal differentiation has not been elucidated. In the present study, TPA-induced epidermal differentiation and hyperplasia were suppressed by inhibition of increases in St2b2 expression, the primary cause of increased CS concentrations after TPA treatment (Figs. 5, 6). CS may be involved in epidermal differentiation through the activation of PKC.[13,30] Combined with our present results obtained with a PKC inhibitor (Fig. 4), TPA-induced PKC activation appears to result from increased St2b2 expression and consequent elevations in CS concentrations.

Our results suggest that TPA-induced increases in CS concentrations cause hyperplasia (Figs. 3, 5, 6). TPA stimulates proliferation and differentiation in skin epidermis *via* activation of several forms of PKC. Knocking down St2b2 expression, and consequent inhibition of CS biosynthesis, likely inhibited epidermal differentiation and blocked hyperplasia. Previous reports showed that successive doses of CS inhibited the tumor-promoting effects of TPA in mouse skin.[30] Chida *et al.* also reported that a single large dose of CS (400 μg) caused desquamation but not proliferation. Together, these results suggest that repeated high doses of CS inhibit TPA-induced tumorigenesis.

The anti-inflammatory agent indomethacin decreased TPA-mediated increases in Ch-ST activity and epidermal hyperplasia.[22,31] This suggested that inflammatory cytokines mediate the enhanced St2b2 expression after TPA treatment. In fact, TNFα did not promote INV expression in the absence of increased St2b2 expression (Fig. 9). In addition, TPA-induced St2b2 expression diminished when TNFα signaling was suppressed (Fig. 10). Inhibiting TNFα binding to TNFR also reduced St2b2 expression (Fig. 11). These results indicated that TNFα triggers St2b2 expression in TPA-induced epidermal hyperplasia and differentiation.

NF-κB is known to participate in TPA-induced epidermal hyperplasia.[32—34] In the present study, an NF-κB inhibitor suppressed TNFα-induced expression of cornified envelope proteins and St2b2 (Fig. 12). These results suggest that TNFα–NF-κB signaling regulates St2b2 expression during TPA-induced epidermal hyperplasia. In fact, a putative NF-κB binding sequence was found in the 5′-flanking region of the St2b2 gene (DNASIS software version 3.0, Hitachi Software Engineering Co., Tokyo, Japan). Therefore, St2b2 expression may increase owing to NF-κB activation of gene transcription. We also identified putative NF-κB binding sequences in the 5′-flanking region of the human Ch-ST ST2B1. In addition, ST2B1 expression increased when the LS174T human epithelial colon carcinoma cell line was treated with TPA or TNFα (unpublished results, Matsuda *et al.*). Thus, NF-κB may be involved in TPA-induced enhancement of ST2B expression in humans as well.

TNFα-siRNA decreased TNFα levels in the medium but not the expression of St2b2 or INV protein in the group not treated with TPA (Fig. 10). Neither TNFR-Ab nor BAY 11-7082 significantly inhibited basal expression levels of St2b2 and INV (Figs. 11, 12). These results suggested that TNFα–NF-κB signaling does not drive constitutive expression of St2b2 and INV, although the mechanisms underlying basal expression of these proteins remain unknown.

In conclusion, St2b2 is required for TPA-induced epidermal hyperplasia, a relationship that involves TNFα–NF-κB signaling. Our hypothesis for the mechanism of TPA-induced epidermal differentiation is shown in Fig. 13. TPA increases TNFα levels to activate NF-κB following binding to TNFR. Then, NF-κB activates St2b2 gene transcription, leading to an increase in the levels of St2b2 and epidermal CS. Finally, increased epidermal CS concentrations enhance the expression of cornified envelope proteins, such as INV, through PKC activation.

Acknowledgements We thank Mr. Hiroyuki Takatoku for technical support.

REFERENCES

1) Ekanayake-Mudiyanselage S., Aschauer H., Schmook F. P., Jensen J. M., Meingassner J. G., Proksch E., *J. Invest. Dermatol.*, **111**, 517—523 (1998).
2) Greenberg C. S., Birckbichler P. J., Rice R. H., *FASEB J.*, **5**, 3071—3077 (1991).
3) Takigawa M., Verma A. K., Simsiman R. C., Boutwell R. K., *Biochem. Biophys. Res. Commun.*, **105**, 969—976 (1982).
4) Castagna M., Takai Y., Kaibuchi K., Sano K., Kikkawa U., Nishizuka Y., *J. Biol. Chem.*, **257**, 7847—7851 (1982).
5) Kikkawa U., Takai Y., Tanaka Y., Miyake R., Nishizuka Y., *J. Biol. Chem.*, **258**, 11442—11445 (1983).
6) Nakadate T., *Jpn. J. Pharmacol.*, **49**, 1—9 (1989).
7) Elias P. M., Williams M. L., Maloney M. E., Bonifas J. A., Brown B. E., Grayson S., Epstein E. H. Jr., *J. Clin. Invest.*, **74**, 1414—1421 (1984).
8) Koppe G., Marinkovic-Ilsen A., Rijken Y., De Groot W. P., Jobsis A. C., *Arch. Dis. Child.*, **53**, 803—806 (1978).
9) Zettersten E., Man M. Q., Sato J., Denda M., Farrell A., Ghadially R., Williams M. L., Feingold K. R., Elias P. M., *J. Invest. Dermatol.*, **111**, 784—790 (1998).
10) Shimada M., Kamiyama Y., Sato A., Honma W., Nagata K., Yamazoe Y., *J. Biochem.*, **131**, 167—169 (2002).
11) Shimada M., Matsuda T., Sato A., Akase T., Matsubara T., Nagata K., Yamazoe Y., *Xenobiotica*, **38**, 1487—1499 (2008).
12) Jetten A. M., George M. A., Pettit G. R., Herald C. L., Rearick J. I., *J. Invest. Dermatol.*, **93**, 108—115 (1989).
13) Kiguchi K., Kagehara M., Higo R., Iwamori M., DiGiovanni J., *J. Invest. Dermatol.*, **111**, 973—981 (1998).
14) Djian P., Phillips M., Easley K., Huang E., Simon M., Rice R. H., Green H., *Mol. Biol. Evol.*, **10**, 1136—1149 (1993).
15) Eckert R. L., Yaffe M. B., Crish J. F., Murthy S., Rorke E. A., Welter J. F., *J. Invest. Dermatol.*, **100**, 613—617 (1993).
16) Crish J. F., Howard J. M., Zaim T. M., Murthy S., Eckert R. L., *Differentiation*, **53**, 191—200 (1993).
17) Watt F. M., *J. Invest. Dermatol.*, **81**, 100s—103s (1983).
18) Kohler H. B., Huchzermeyer B., Martin M., De Bruin A., Meier B., Nolte I., *Vet. Dermatol.*, **12**, 129—137 (2001).
19) Sen C. K., Packer L., *FASEB J.*, **10**, 709—720 (1996).
20) Murakawa M., Yamaoka K., Tanaka Y., Fukuda Y., *Biochem. Pharmacol.*, **71**, 1331—1336 (2006).
21) Scott K. A., Moore R. J., Arnott C. H., East N., Thompson R. G., Scallon B. J., Shealy D. J., Balkwill F. R., *Mol. Cancer Ther.*, **2**, 445—451 (2003).
22) Yamamoto S., Jiang H., Kato R., *Carcinogenesis*, **12**, 1145—1147 (1991).
23) Bradford M. M., *Anal. Biochem.*, **72**, 248—254 (1976).
24) Xu X. X., Lambeth J. D., *J. Biol. Chem.*, **264**, 7222—7227 (1989).
25) Chen G., Goeddel D. V., *Science*, **296**, 1634—1635 (2002).
26) Dlugosz A. A., Mischak H., Mushinski J. F., Yuspa S. H., *Mol. Carcinog.*, **5**, 286—292 (1992).
27) Ohba M., Ishino K., Kashiwagi M., Kawabe S., Chida K., Huh N. H., Kuroki T., *Mol. Cell. Biol.*, **18**, 5199—5207 (1998).
28) Osada S., Mizuno K., Saido T. C., Akita Y., Suzuki K., Kuroki T., Ohno S., *J. Biol. Chem.*, **265**, 22434—22440 (1990).
29) Zhang G., Kazanietz M. G., Blumberg P. M., Hurley J. H., *Cell*, **81**, 917—924 (1995).
30) Chida K., Murakami A., Tagawa T., Ikuta T., Kuroki T., *Cancer Res.*, **55**, 4865—4869 (1995).
31) Fischer S. M., Gleason G. L., Mills G. D., Slaga T. J., *Cancer Lett.*, **10**, 343—350 (1980).
32) Amigo M., Paya M., Braza-Boils A., De Rosa S., Terencio M. C., *Life Sci.*, **82**, 256—264 (2008).
33) Lizzul P. F., Aphale A., Malaviya R., Sun Y., Masud S., Dombrovskiy V., Gottlieb A. B., *J. Invest. Dermatol.*, **124**, 1275—1283 (2005).
34) Seitz C. S., Lin Q., Deng H., Khavari P. A., *Proc. Natl. Acad. Sci. U.S.A.*, **95**, 2307—2312 (1998).

Molecular Genetics and Metabolism 102 (2011) 91–98

Contents lists available at ScienceDirect

Molecular Genetics and Metabolism

journal homepage: www.elsevier.com/locate/ymgme

Functional analysis of genetic variations in the 5′-flanking region of the human MDR1 gene

Mayumi Saeki, Kouichi Kurose, Ryuichi Hasegawa, Masahiro Tohkin *

Division of Medicinal Safety Science, National Institute of Health Sciences, 1-18-1 Kamiyoga, Setagaya-ku, Tokyo 158-8501, Japan

ARTICLE INFO

Article history:
Received 26 August 2010
Accepted 26 August 2010
Available online 19 September 2010

Keywords:
5′-flanking region
Multidrug resistance 1
Nuclear receptors
P-glycoprotein
Single nucleotide polymorphism

ABSTRACT

P-glycoprotein (P-gp), the product of the *MDR1* gene, shows large interindividual variations in expression, which leads to differences in the pharmacokinetics of the substrate drugs. The functions of single nucleotide polymorphisms located in the nuclear receptor-responsive element of the 5′-flanking region in the human *MDR1* gene were analyzed in order to clarify the mechanism underlying the interindividual variation in P-gp expression. Electrophoretic mobility shift assays revealed that the −7833C>T substitution in the nuclear receptor-responsive region of *MDR1* decreases the binding affinities of four nuclear receptors to their responsive elements: vitamin D receptor (VDR), thyroid hormone receptor (TR), constitutive androstane receptor (CAR), and pregnane X receptor (PXR). A reporter gene assay revealed that the C-to-T substitution at −7833 also reduces the transcriptional activation of *MDR1* by VDR, TRβ, CAR, and PXR. However, another SNP (−1211T>C substitution), which results in the formation of a xenobiotic responsive element-like sequence and a hypoxia responsive element-like sequence, failed to affect the aryl hydrocarbon receptor-dependent and hypoxia-induced transcriptional activation of *MDR1*. Although the frequency of the −7833C>T substitution in *MDR1* is relatively low, the SNP is crucial because it may alter the pharmacokinetics of P-gp substrates in a small subset of the population.

1. Introduction

P-glycoprotein (P-gp) transports a wide variety of compounds, including foreign xenobiotics and endogenous substrates, to the outside of cells [1,2]. P-gp is encoded by the human *MDR1* gene and is expressed in various physiological barriers such as intestinal epithelium [3,4], kidney tubules cells [3], the liver [3], and the capillary endothelium of the central nervous system [5]. It also plays an important role in pharmacokinetic processes such as drug absorption [1,6–8], renal secretion [9], biliary excretion [10], and brain distribution [11–13]. The large interindividual variations in P-gp expression and activity levels [14–17] suggest that the systemic exposure level and tissue concentrations of drugs that are P-gp substrates vary depending on the subject [15,18]. The pharmacokinetic differences ultimately lead to interindividual variation in drug efficacy and adverse reactions. Therefore, P-gp expression levels and activity are crucial factors in drug efficacy and safety.

The results of several studies suggest that the basis of interindividual variation in P-gp expression and activity resides in the presence of single nucleotide polymorphisms (SNPs) in the coding region of *MDR1* [2,19–22]. Hoffmeyer et al. showed that 3435C>T, a synonymous SNP in exon 26, is associated with reduced P-gp expression in the duodenum and increased plasma levels of digoxin, a typical P-gp substrate, following its oral administration to healthy volunteers [23].Wang et al. also reported that 3435C>T appears to affect the allelic variation of MDR1 expression in the liver via a change in mRNA stability [24]. In addition to digoxin, other studies have reported that the T allele of 3435C>T is related to higher plasma concentrations of cyclosporine A. While these reports suggest the importance of *MDR1* exonic SNPs in the regulation of P-gp expression, conflicting results have been reported [18,23,25–27].

In addition to SNPs in the coding region, there are variations in the 5′-flanking region that could affect *MDR1* gene transcription and mRNA expression levels. Haplotypes in the *MDR1* transcriptional regulatory region suggest the existence of functional haplotypes that could alter P-gp expression [17,28,29]. In these studies, the −1789G>A haplotype, alone or in combination with −145C>G, was associated with decreased P-gp expression. However, the reported effects on P-gp expression of haplotypes carrying −129T>C and two other linked SNPs were contradictory, showing reduction and enhancement [27,30,31]. These reports suggest that functional SNPs in the 5′-flanking region have not been fixed, and the relationship between these SNPs and the transcriptional factors that regulate the *MDR1* gene transcription is unknown. Therefore, the mechanism underlying interindividual variations in the expression levels of P-gp remains unclear.

Geick et al. found that the induction of MDR1 mRNA by rifampicin is mediated by pregnane X receptor (PXR), which binds to direct

* Corresponding author. Fax: +81 3 3700 9788.
E-mail address: tohkin@nihs.go.jp (M. Tohkin).

1096-7192/$ - see front matter © 2010 Elsevier Inc. All rights reserved.
doi:10.1016/j.ymgme.2010.08.019

repeat sequences separated by four bases (DR4) located −7.9 to −7.8 kbp upstream of the transcription start site [32]. This region contains several DR sequences and functions as the enhancer region in *MDR1* [32]. The constitutive androstane receptor (CAR) also induces MDR1 mRNA expression by binding to several DR4s located in the same region [33]. Recently, we reported that the thyroid hormone receptor β (TRβ) and vitamin D receptor (VDR) regulate the expression of *MDR1* by binding to several DRs located in this region [34,35]. A SNP, −7833C>T, has been reported within one of the half-sites (Hs), a pair of which composes a DR or ER (AGTTCA>AGTTTA,

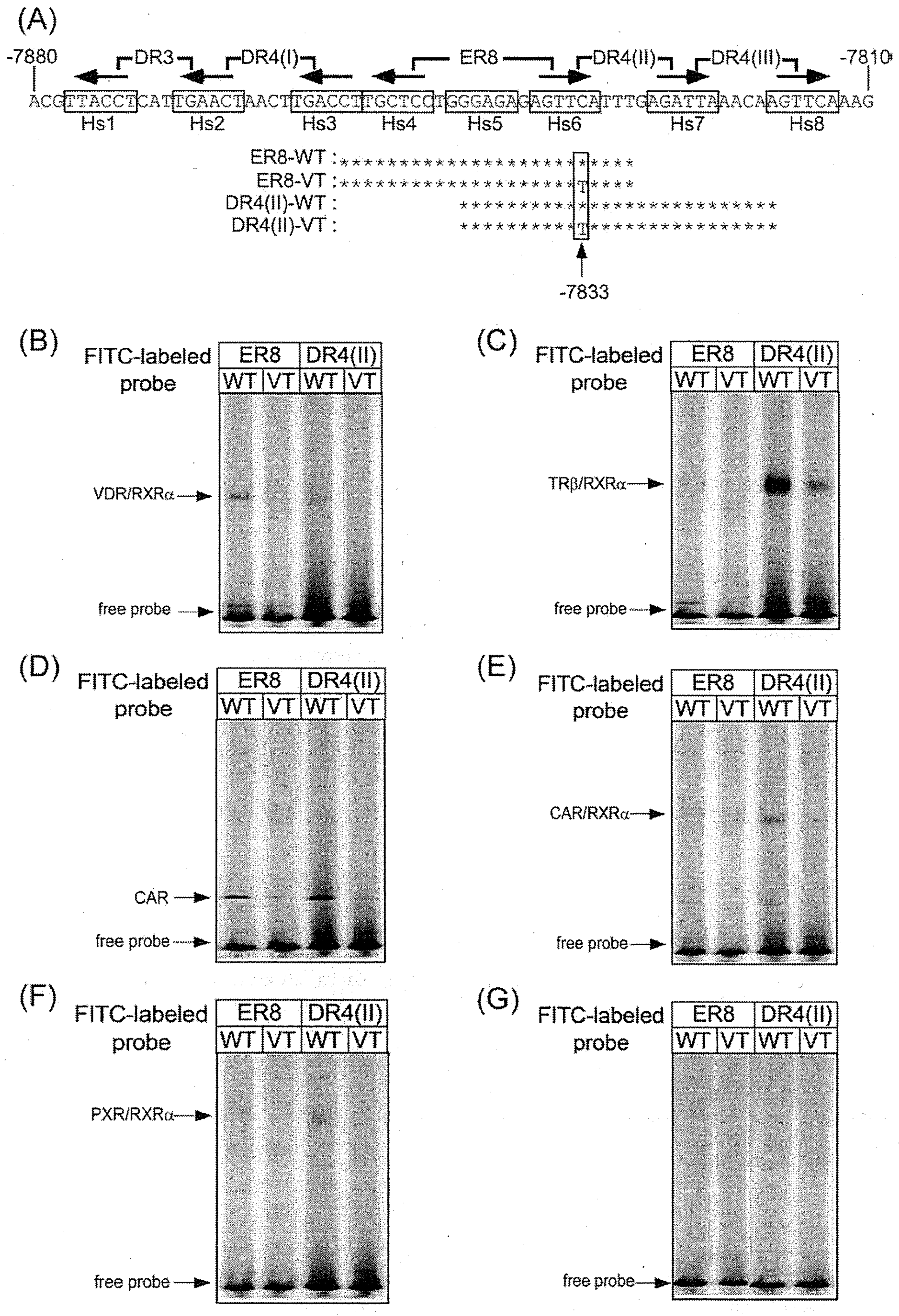

Fig. 1. The C-to-T substitution at −7833 affects the binding affinity of nuclear receptors to ER8 and/or DR4(II) in the *MDR1* gene. (A) Oligonucleotide sequences used for the electrophoretic mobility shift assay (EMSA). Several half-sites (designated as Hs1 to 8 in this study) are boxed, and arrows indicate the direction of the half-site. The C-to-T substitution at −7833 is located within Hs6. The numbers are in reference to the transcriptional start site at +1. Schematic representations of probes containing the −7833C (ER8-WT and DR4(II)-WT) or −7833T (ER8-VT and DR4(II)-VT) allele are shown. Only nucleotides that differ from the wild-type are shown as letters; asterisks represent unchanged nucleotides. (B) EMSA was performed using *in vitro* translated VDR and RXRα. The FITC-labeled probe was incubated with VDR and RXRα as described in the Materials and methods. The complexes were resolved by electrophoresis on a 6% Long Ranger gel. This protocol was also used for the EMSAs shown in C–G. (C) EMSA was performed using *in vitro* translated TRβ and RXRα. (D) EMSA was performed using *in vitro* translated CAR. (E) EMSA was performed using *in vitro* translated CAR and RXRα. (F) EMSA was performed using *in vitro* translated PXR and RXRα. (G) We carried out the translation reaction using the empty vector, and performed EMSA using the reaction product instead of *in vitro* translated nuclear receptors, as the negative control.

Fig. 1A) [9,36]. Although the frequency of this substitution is very low (0.002), there is the possibility the −7833C>T variant may influence the transcription of the *MDR1* gene.

MDR1 mRNA expression was also induced by 2,3,7,8-tetrachlorodibenzo-p-dioxin (aryl hydrocarbon receptor (AhR) ligand) in three of seven primary human hepatocytes [37], an indication of the interindividual variation in AhR-induced expression, although the AhR responsive element (xenobiotics responsive element; XRE) in *MDR1* has not been identified. The −1211T>C (rs28746504, −1910 in Taniguchi et al., [17] and −1017 in Takane et al. [29]) SNP has been found in Japanese and Caucasian populations at allelic frequencies of 0.08–0.1 (Japanese) and 0.016 (Caucasian). The T-to-C substitution at nucleotide −1211 results in an XRE-like sequence (possible XRE, TGGTGTG>TGGCGTG, Fig. 3A) that we hypothesize may cause the interindividual variability in the response to TCDD. In addition to AhR-induced MDR1 mRNA expression, hypoxia-inducible factor-1 (HIF-1) regulates *MDR1* gene transcription [38]. The −1211T>C substitution also results in an HIF-1-responsive element (hypoxia responsive elements; HRE)-like sequence (possible HRE, GTGTG>GCGTG, Fig. 3A). However, it was unknown if HIF-1 could bind the candidate HRE in addition to the known HRE located between −49 and −45 (−53 and −49 in this study) in the promoter region of *MDR1*.

In order to clarify the functional significance of variants in the transcriptional regulatory region of *MDR1* gene, the effect of two SNPs (−7833C>T and −1211T>C) on the binding properties of nuclear receptors and on the transcriptional activity of *MDR1* was evaluated using electrophoretic mobility shift assay (EMSA) and a luciferase-reporter gene assay, respectively. The −7833C>T substitution resulted in a decrease in nuclear receptor binding and transcriptional activation *in vitro*, while the −1211T>C substitution did not produce an effect. These results suggest that the −7833C>T substitution influences the regulation of MDR1 mRNA levels through PXR, CAR, TRβ, and VDR.

2. Materials and methods

2.1. Chemicals

Rifampicin and 3-methylcholanthrene (3MC) were purchased from Wako Pure Chemicals (Osaka, Japan). $CoCl_2$, 3,3′,5-triiodo-L-thyronine (T3), and 1α,25-dihydroxyvitamin D_3 (1,25-$(OH)_2D_3$) were purchased from Sigma-Aldrich (St. Louis, MO, USA). All chemicals, except T3 and $CoCl_2$, were dissolved in dimethyl sulfoxide (DMSO). T3 and $CoCl_2$ were dissolved in 0.2 M NaOH and water, respectively.

2.2. Plasmid constructs

The expression plasmids, pDEST12.2-hPXR, pEF6/V5-hVDR, pCMVTNT-hVDR, and pcDNA3.1-TRβ, were previously constructed in our laboratory [34,35,39]. The expression plasmid encoding human RXRα cDNA (pcDNA3.1-hRXRα) was a generous gift from Dr. Shuichi Koizumi (Yamanashi University, Japan). pCMVTNT-hTRβ was constructed by ligating the *Eco*RI/*Not*I fragment from pcDNA3.1-TRβ into the pCMVTNT expression plasmid (Promega, Madison, WI, USA), which was digested with *Eco*RI and *Not*I. The pEGFP-hCAR was a generous gift from Dr. Hideto Jinno (National Institute of Health Sciences, Japan) [40]. The nucleotide at the position 540 of pEGFP-hCAR differed from the reference sequence (NM_005122) (540C>T, synonymous substitution) [40]. Thus, wild-type sequence was introduced into the pEGFP-hCAR using a QuikChange Site-Directed Mutagenesis Kit (Stratagene, La Jolla, CA, USA). pEGFP-hCAR was then digested with *Xho*I and *Eco*RI, and the resulting fragment was ligated into the pcDNA3.1/Zeo expression plasmid (Invitrogen, Carlsbad, CA, USA), which was digested with *Xho*I and *Eco*RI. This expression plasmid (pcDNA3.1-hCAR) was digested with *Xho*I and *Pme*I, and the resulting fragment was ligated into the pCMVTNT expression plasmid, which was digested with *Xho*I and *Sma*I (pCMVTNT-hCAR). The pDEST12.2-hPXR, pEF6/V5-hVDR, pcDNA3.1-TRβ, and pcDNA3.1-hCAR plasmids were used for transfections. The pDEST12.2-hPXR, pCMVTNT-hVDR, pCMVTNT-hTRβ, pCMVTNT-hCAR, and pcDNA3.1-hRXRα plasmids were used for *in vitro* synthesis.

The luciferase reporter gene plasmids, pMD10082L, pMD*824Δ90L, and pMD457L were previously constructed in our laboratory [34]. The pMD2912L plasmid was constructed by deleting the *Nsi*I fragment from pMD10082L. Mutations were introduced at positions −7833 and −1211 of pMD*824Δ90L-WT and pMD2912L-WT to create pMD*824Δ90L-VT and pMD2912L-VT, respectively, using a QuikChange Multi Site-Directed Mutagenesis Kit (Stratagene), according to the manufacturer's instructions, with the following oligonucleotides:

−7833C>T_SNP: 5′-GCTCCTGGGAGAGAGTTTATTTGAGATTAAACAAG-3′

−1211T>C_SNP: 5′-CAGGAGAATGGCGTGAACCCGGGAG-3′.

The pGL2A8-2504 [41] plasmid, which contains the XRE of the Syrian hamster CYP2A8, was digested with *Kpn*I and *Hin*dIII. The resulting fragment was ligated to the *Kpn*I/*Hin*dIII site of the firefly luciferase rapid response reporter vector pGL4.12 (Promega). This plasmid (pGL4.12-2A8) was used as a positive control.

2.3. Electrophoretic mobility shift assay (EMSA)

TNT T7 Quick Coupled Transcription/Translation Systems (Promega) were used for *in vitro* synthesis of human RXRα protein from pcDNA3.1-hRXRα, according to the manufacturer's instructions. TNT SP6 Quick Coupled Transcription/Translation Systems (Promega) were used for *in vitro* synthesis of human VDR, TRβ, CAR, and PXR proteins from pCMVTNT-hVDR, pCMVTNT-hTRβ, pCMVTNT-hCAR, and pDEST12.2-hPXR, respectively, according to the manufacturer's instructions. The plus strand sequences of probes used in the EMSAs are shown in Fig. 1A. The oligonucleotides were purchased from Sigma Genosys (Hokkaido, Japan) and equal amounts of complimentary strands were annealed. The reaction mixture was prepared as follows: a 2.5 μL aliquot of the *in vitro* translated proteins (nuclear receptor alone, or mixed at a ratio of 1:1) or unprogrammed reticulocyte lysate was incubated for 20 min at room temperature with 1 μL of 5× binding buffer (15 mM $MgCl_2$, 0.5 mM EDTA, 2.5 mM dithiothreitol (DTT), 50% glycerol and 100 mM HEPES, pH 7.75), 0.5 μL of 1 mg/mL poly(dI–dC) (GE Healthcare, Little Chalfont, UK), and 0.5 μL of 0.33 μM 5′-fluorescein isothiocyanate (FITC)-labeled double stranded oligonucleotide probe. The protein–DNA complexes were resolved by electrophoresis on 6% non-denaturing Long Ranger gels (Lonza, Rockland, ME) run in 0.5×TBE (44.5 mM Tris, 44.5 mM boric acid, and 1.25 mM EDTA) at 500 V constant voltage, and visualized and quantified on a slab gel DNA sequencer (DSQ-2000L; Shimadzu Co., Kyoto, Japan).

2.4. Cell culture

Caco-2 cells, a human colon adenocarcinoma cell line, were obtained from the American Type Culture Collection (Manassas, VA, USA). Caco-2 cells were cultured in low glucose Dulbecco's modified Eagle's medium (DMEM, Sigma-Aldrich) supplemented with 10% heat-inactivated fetal bovine serum (FBS), 100 U/mL penicillin G/100 μg/mL streptomycin (Gibco-Invitrogen, Carlsbad, CA, USA), and 1× MEM non-essential amino acids solution (Gibco-Invitrogen) at 37 °C under 5% CO_2–95% air.

2.5. Transfection and luciferase reporter gene assays

Caco-2 cells were seeded into 96-well plates (1.7×10^4 cells/well), grown overnight, and transiently transfected using HilyMax (at a ratio of DNA to HilyMax of 1:5; Dojindo Laboratories, Kumamoto, Japan) according to the manufacturer's instructions with 10 ng/well of the indicated expression plasmid, 100 ng/well of the indicated luciferase reporter plasmid, and 10 ng/well of the *Renilla* luciferase reporter plasmid, pGL4.74 [hRluc/TK] (Promega) to normalize the transfection efficiency. After 24 h, the medium was replaced by phenol red-free DMEM (Gibco-Invitrogen) supplemented with 10% dextran-coated charcoal-stripped FBS (Hyclone Laboratories, Logan, UT, USA) containing 1 μM 3MC, 150 μM $CoCl_2$, 25 nM 1,25-$(OH)_2D_3$, 50 nM T3, 10 μM rifampicin, or vehicle (DMSO, water, or 0.2 mM NaOH) for 3.5 h except for $CoCl_2$. $CoCl_2$ treatment was performed for 6 h. Firefly and *Renilla* luciferase activities were measured using the Dual-Glo Luciferase Assay System (Promega) according to the manufacturer's instructions and a luminometer (Wallac 1420 ARVO sx Multilabel Counter, Perkin-Elmer Life Sciences, Boston, MA, USA). Firefly luciferase activity was normalized to *Renilla* luciferase activity (Luc activity). The inducibility (fold induction) was calculated as the ratio of luciferase activity of ligand-treated cells to that of control cells. As for CAR, fold transactivation was calculated as the ratio of luciferase activity of CAR-transfected cells to that of pcDNA3.1 transfected cells. The results were presented as the mean ± standard deviation (S.D.) of at least four independent experiments. The statistical analysis was performed using two-tailed, unpaired t-tests with a significance level of $P<0.05$.

3. Results

3.1. C-to-T substitution at −7833 of MDR1 decreases binding affinity of nuclear receptors to ER8 and/or DR4(II)

Nuclear receptors, such as VDR, TRβ, CAR, and PXR reportedly up-regulate *MDR1* expression through the response region located 7880 to 7810 bp upstream of the *MDR1* gene. This region contains several half-sites, a pair of which composes a DR or ER (Hs1–8 in Fig. 1A). The previously reported variation −7833C>T is located within the Hs6 half-site (Fig. 1A). The effect of the C-to-T substitution at −7833 on the binding affinity of nuclear receptors to the response region was examined with EMSA using *in vitro* translated VDR, TRβ, PXR, CAR and RXRα. ER8 and DR4(II) oligonucleotide probes containing either −7833C (WT) or −7833T (VT) were used because Hs6 is involved in both ER8 and DR4(II) (Fig. 1A). The probes used for the EMSA are summarized in Fig. 1A. As described in previous reports, VDR/RXRα forms DNA–protein complexes with ER8-WT and DR4(II)-WT, with a weaker binding affinity for DR4(II) than for ER8. Introduction of the variant into the probes (DR4(II)-VT and ER8-VT) decreased the formation of VDR/RXRα and probe complexes (Fig. 1B). As described previously, the DNA-TRβ/RXRα complex was formed using DR4(II)-WT, but not with ER8-WT (Fig. 1C). The DR4(II)-TRβ/RXRα complex significantly decreased when the variant type probe (DR4(II)-VT) was used. It has been reported that CAR binds to Hs6 as a monomer [33]. Consistent with this report, the DNA–CAR monomer complex was formed with either ER8-WT or DR4(II)-WT, and the C-to-T substitution at −7833 (ER8-VT and DR4(II)-VT) caused a decrease in band formation (Fig. 1D). The CAR/RXRα DNA–protein complex was also formed when either ER8-WT or DR4(II)-WT was used as a probe, although the binding affinity of ER8-CAR/RXRα was weak (Fig. 1E). Complex formation between CAR/RXRα and the probes decreased when the WT probes were replaced with ER8-VT and DR4(II)-VT (Fig. 1E). PXR/RXRα DNA–protein complexes formed using both ER8-WT and DR4(II)-WT produced weak bands, which disappeared when ER8-VT and DR4(II)-VT were used as probes (Fig. 1F). These results indicate that the C-to-T substitution at −7833 leads to decreased binding affinity of ER8 and/or DR4(II) for VDR/RXRα, TRβ/RXRα, CAR, CAR/RXRα, and PXR/RXRα.

3.2. C-to-T substitution at −7833 of MDR1 affects the inducibility by 1,25-$(OH)_2D_3$, T3, CAR, and PXR, but does not affect the inducibility by rifampicin

The EMSA experiments revealed that the C-to-T substitution at −7833 results in decreased binding affinity of VDR/RXRα, TRβ/RXRα, CAR, CAR/RXRα, and PXR/RXRα for ER8 and/or DR4(II). To investigate the effect of the substitution on VDR-, TRβ-, CAR-, and PXR-induced *MDR1* transcription, −7833C>T was introduced into pMD*824Δ90L reporter plasmid, which contains the nuclear receptor-response region (Fig. 2A), and a luciferase reporter assay was performed using the Caco-2 intestinal epithelial cell line. In order to exclude the interaction of other nuclear receptors, we used the Caco-2 because Caco-2 cells express the nuclear receptors at relatively lower levels. As described in previous reports [34,35], 1,25-$(OH)_2D_3$ (VDR ligand) or triiodothyronine (T3, TRβ ligand) increased the luciferase activity in Caco-2 cells that were co-transfected with VDR or TRβ expression plasmid (Figs. 2B and C) although VDR or TRβ alone could not activate the transcriptional activity without the ligand (data not shown). The C-to-T substitution resulted in significantly reduced transcriptional activation by 1,25-$(OH)_2D_3$ (Fig. 2B, $P=0.0015$, unpaired t-test, two-tailed). The substitution also led to a slight decrease in T3-induced transcriptional activation, but this decrease was not significant (Fig. 2C, $P=0.0688$, unpaired t-test, two-tailed). Co-transfection of a CAR expression plasmid led to increased transcriptional activity of the reporter gene compared with the mock transfection control group (fold transactivation in Fig. 2D) due to the constitutive activity of CAR. The C-to-T substitution also partially reduced constitutive CAR transactivity (Fig. 2D, $P=0.0326$, unpaired t-test, two-tailed). Rifampicin increased transactivation of the reporter gene following transfection with the PXR expression plasmid. The −7833C>T substitution did not affect the fold induction produced by rifampicin (Fig. 2E). However, the substitution reduced both the rifampicin-dependent and -independent transcriptional activation by PXR (Fig. 2F). These results indicated that −7833C>T in the *MDR1* gene reduced the transcriptional activation which is induced by 1,25-$(OH)_2D_3$

Fig. 2. Effect of −7833C>T on the transactivation of *MDR1* by VDR, TRβ, CAR, and PXR. (A) The C-to-T mutation at −7833 was introduced into a reporter gene plasmid containing the 5′ upstream region from −7880 to −7810 bp of *MDR1* (pMD*824Δ90L). Several half-sites (designated as Hs1 to Hs8) are boxed and arrows indicate the direction of the half-site. The C-to-T substitution at −7833 is located within Hs6. The numbers are in reference to the transcriptional start site at +1. In the variant construct (pMD*824Δ90L-VT), only the nucleotide that differs from the wild-type (pMD*824Δ90L-WT) is shown as a letter; asterisks represent unchanged nucleotides. (B) Caco-2 cells were co-transfected with the indicated luciferase reporter plasmid, VDR expression plasmid, and the *Renilla* luciferase reporter plasmid, and were subsequently treated with DMSO or 1,25-$(OH)_2D_3$. Firefly luciferase activity was normalized to *Renilla* luciferase activity, and the fold induction was calculated as the ratio of luciferase activity in 1,25-$(OH)_2D_3$-treated cells to that of DMSO-treated cells. Each value represents the mean ± S.D. of independent seven experiments. Statistical analysis was performed using a two-tailed, unpaired t-test, and a statistically significant difference, as compared with the wild-type, is indicated by an asterisk (**$P<0.005$). (C) The luciferase assay was performed as described in (B) except that the TRβ expression plasmid, T3, and 0.2 mM NaOH were used instead of the VDR expression plasmid, 1,25-$(OH)_2D_3$, and DMSO, respectively. The fold induction was calculated as the ratio of luciferase activity in T3-treated cells to that in 0.2 mM NaOH-treated cells. Each value represents the mean ± S.D. of independent six experiments. Statistical analysis was performed using the two-tailed, unpaired t-test, ($P=0.069$). (D) Luciferase activity was analyzed as described in the Materials and methods. Firefly luciferase activity was normalized to *Renilla* luciferase activity, and the fold transactivation was calculated as the ratio of luciferase activity of CAR-transfected cells to that of control plasmid-transfected cells. Each value represents the mean ± S.D. of independent four experiments. Statistical analysis was performed using the two-tailed, unpaired t-test, and a statistically significant difference, as compared with the wild-type, is indicated by asterisk (*$P<0.05$). (E) The luciferase assay was performed as described in (B) except that PXR expression plasmid and rifampicin were used instead of VDR expression plasmid and 1,25-$(OH)_2D_3$, respectively. The fold induction was calculated as the ratio of luciferase activity in rifampicin-treated cells to that in DMSO-treated cells. Each value represents the mean ± S.D. of independent five experiments. (F) These data are from the experiments described in (E), but are expressed in each treatment group. The firefly luciferase activity was normalized for transfection efficiency, using the activity of co-transfected *Renilla* luciferase, and represented as Luc activity.

and T3. The −7833C>T also reduced CAR and PXR-dependent transcriptional activities.

3.3. XRE- and HRE-like sequences, resulting from a −1211T>C substitution in MDR1, are not functional

The T-to-C substitution at −1211 from the transcriptional start site of the human *MDR1* gene (−1211T>C, rs28746504) results in the formation of a XRE-like sequence (TGGTGTG>TGGCGTG, Fig. 3A). To examine the functionality of the XRE-like sequence, −1211T>C was introduced into a reporter plasmid containing the 5′ upstream region from −2912 to +117 bp of the *MDR1* gene and transfected into Caco-2 cells. The pGL4.12-2A8 construct (2A8), which contains the functional XRE, was used as the positive control [41]. As shown in Fig. 3B, 3MC (AhR ligand) did not affect transcriptional activity of Caco-2 cells transfected with either the wild-type (pMD2912L-WT) or mutated (pMD2912L-VT) construct, although the luciferase activity of the positive control reporter construct (2A8) was increased approximately 5-fold by 3MC, indicating that the XRE-like sequence containing −1211T>C is not functional.

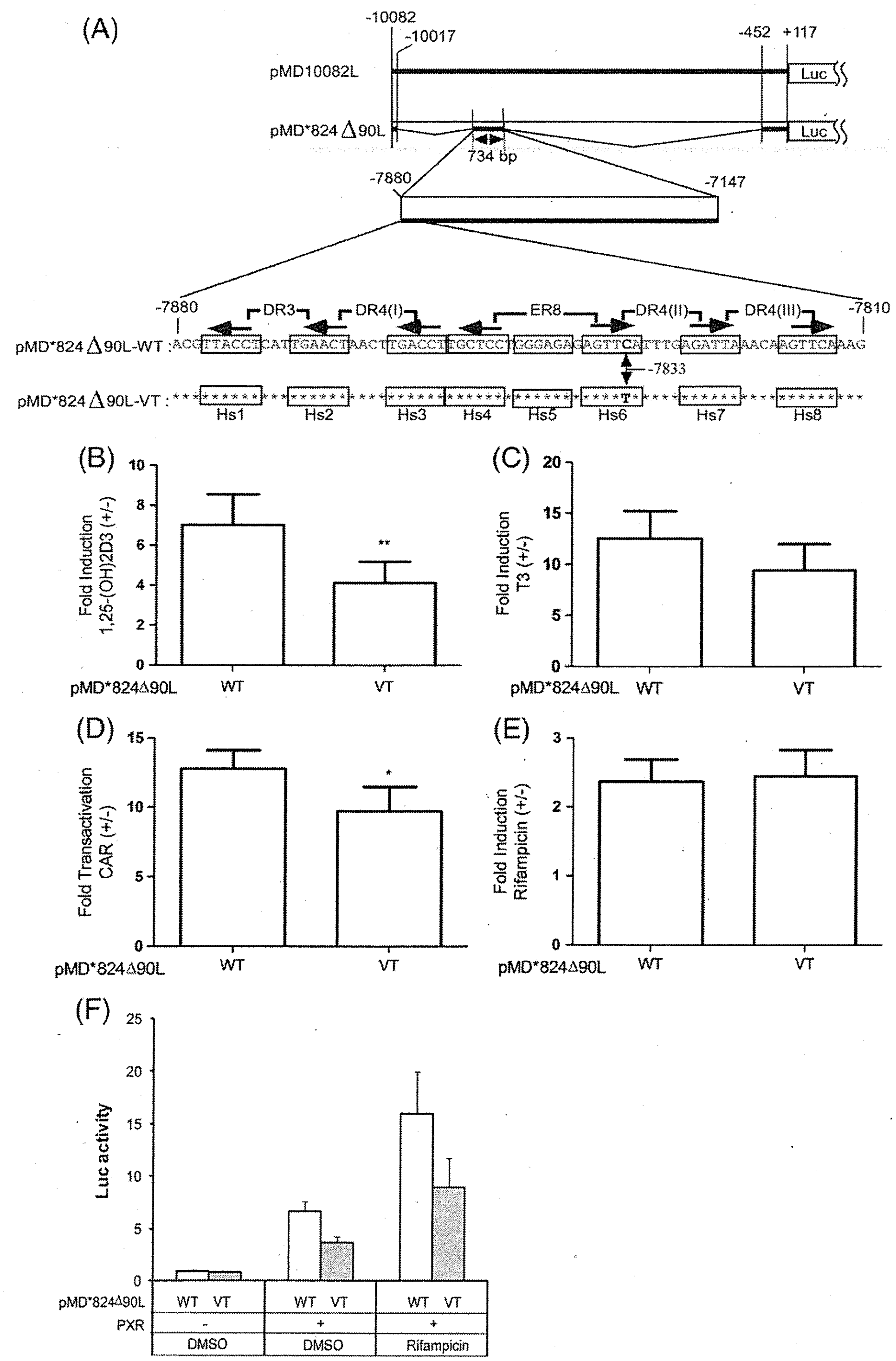

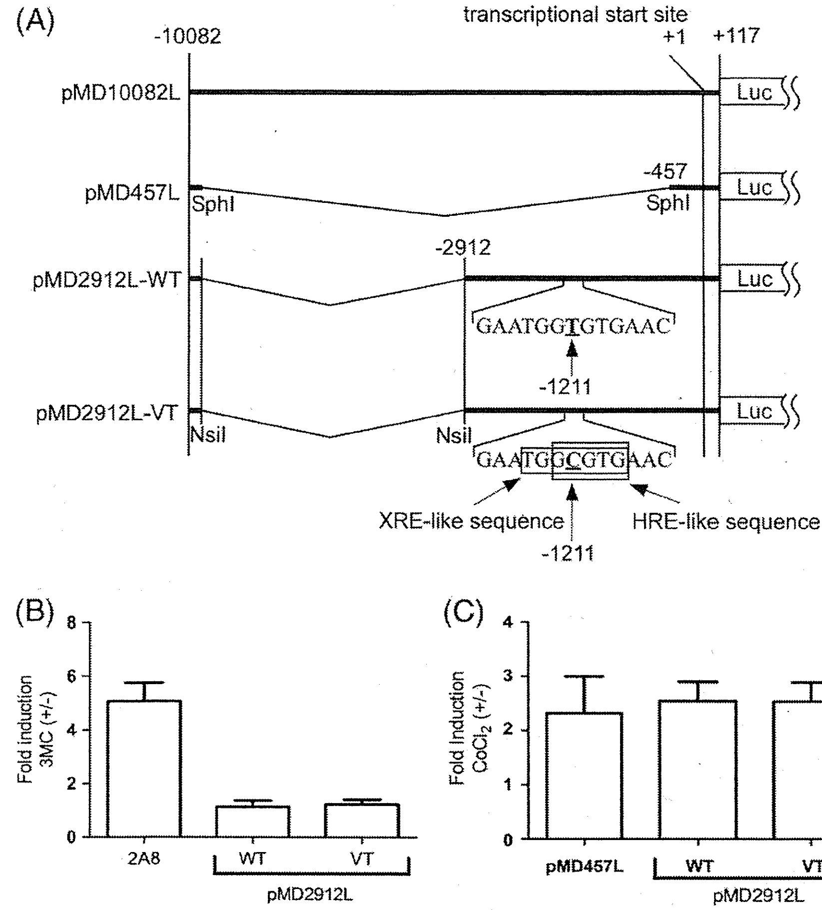

Fig. 3. Effect of −1211T>C on the transactivation of the *MDR1* gene by AhR and HIF. (A) Schematic representation of reporter plasmids containing the −1211T (pMD2912L-WT) or −1211C (pMD2912L-VT) allele. The pMD2912L plasmid was constructed by deleting the *Nsi*I fragment in pMD10082L. The numbers are in reference to the transcriptional start site at +1. Xenobiotic response element (XRE)-like and hypoxia response element (HRE)-like sequences (TGGCGTG and GCGTG, respectively) resulting from the T-to-C substitution at −1211 are boxed. pMD457L was constructed by deleting the *Sph*I fragment from pMD10082L. (B) Caco-2 cells were co-transfected with the indicated luciferase reporter plasmid and the *Renilla* luciferase reporter plasmid, and were subsequently treated with DMSO or 3MC as described in Materials and methods. Firefly luciferase activity was normalized to *Renilla* luciferase activity, and the fold induction was calculated as the ratio of luciferase activity in 3MC-treated cells to that in DMSO-treated cells. As a positive control, pGL4.12-2A8 (2A8), which contains the functional XRE of Syrian hamster CYP2A8, was used. Each value represents the mean ± S.D. of four independent experiments. (C) Caco-2 cells were co-transfected with the indicated luciferase reporter plasmid and the *Renilla* luciferase reporter plasmid, and then replaced by media with or without $CoCl_2$ as described in Materials and methods. Firefly luciferase activity was normalized to *Renilla* luciferase activity, and the fold induction was calculated as the ratio of luciferase activity in $CoCl_2$-treated cells to that of untreated cells. The pMD457L, which contains the functional HRE but does not contain the HRE-like sequence, was used as a control. Each value represents the mean ± S.D. of four independent experiments.

The T-to-C substitution at −1211 also results in the formation of an HRE-like sequence (GTGTG>GCGTG, Fig. 3A). The effect of the −1211T>C mutation on hypoxia responsiveness was measured by transfecting Caco-2 cells with the pMD2912L-WT or pMD2912L-VT. The cells were cultured with or without $CoCl_2$, a hypoxia-mimetic agent [38]. As shown in Fig. 3C, $CoCl_2$-dependent inducibility of the wild-type construct (pMD2912L-WT) was similar to that of the variant construct (pMD2912L-VT). Moreover, the inducibility of the wild-type construct, which includes the HRE-like sequence and the known HRE between −53 and −49, was also similar to that of pMD457L, which contains the reported functional HRE alone [38]. Therefore, the −1211T>C substitution did not affect the hypoxic response, and the HRE-like sequence is also non-functional.

4. Discussion

Many studies have tried to clarify the relationship between P-gp expression levels and SNPs located in the coding and transcriptional regulatory regions of *MDR1* [2,19,21–23,28,42]. However, most of these studies have not explored the functionality of these SNPs based on the nuclear receptor-responsive elements that play important roles in the expression of MDR1 mRNA. Therefore, the proposed functions of SNPs in the 5′-flanking region, such as −129T>C, remain controversial [27,30,31]. In this study, we analyzed the SNP located in the nuclear receptor-responsive region of *MDR1* and the SNP that results in conversion to a potential nuclear receptor-responsive element. The −7833C>T substitution, located in the nuclear receptor-responsive region, was found to significantly decrease the binding affinity of VDR/RXRα, TRβ/RXRα, CAR, CAR/RXRα, and PXR/RXRα (Fig. 1). In addition, the −7833C>T substitution reduced the transcriptional activation induced by 1,25-$(OH)_2D_3$ and T3, and suppressed CAR and PXR-dependent transcriptional activities *in vitro* (Fig. 2).

Recently, we reported that the relative binding ability of VDR/RXRα to the elements located in this region is: DR4(I)>DR3>ER8(MdC3)>DR4(III)>DR4(II), and DR4(I), with ER8(MdC3), and DR4(III) the main players in VDR-mediated MDR1 induction [35]. Since −7833C>T is involved in ER8(MdC3) (Fig. 1A), and ER8(MdC3) contributes to VDR-mediated MDR1 induction [35], it is possible that the −7833C>T substitution decreases VDR-mediated MDR1 mRNA induction through ER8(MdC3). We also previously indicated that TRβ/RXRα bound to several DRs in the order: DR4(I)>DR4(II)>DR3≈DR4(III), and that every direct repeat contributes to TRβ-mediated MDR1 induction [34]. Since −7833C>T is located in DR4(II) (Fig. 1A), and TRβ/RXRα can bind to DR4(II) at a relative high affinity [34], it is reasonable that the −7833C>T substitution could affect TRβ-mediated MDR1 mRNA induction though DR4(II). Burk et al. reported that CAR binds DR4(I) and DR4(III) as a heterodimer with RXRα, and to the 5′ half-site of DR4(II) (designated as Hs6 in Fig. 1A) as a CAR monomer, and suggested that DR4(I) and the 5′ half-site of DR4(II) (Hs6) were important elements for the CAR-mediated MDR1 induction [33]. In this study, the CAR monomer formed a complex with Hs6 both in ER8(MdC3) and DR4(II), and CAR/RXRα formed a complex with DR4(II) (Figs. 1D and E). These results and those of Burk indicate that Hs6 contributes to the CAR-mediated MDR1 mRNA induction. Since −7833C>T is found in Hs6 and DR4(II) (Fig. 1A), the −7833C>T substitution could decrease CAR-mediated MDR1 mRNA induction (Fig. 2D) even if the CAR monomer or CAR/RXRα contributes to MDR1 mRNA induction. Geick et al. reported that PXR/RXRα bind to DR4(I), DR4(II), and DR4(III) in the nuclear receptor-responsive elements of *MDR1*, with the highest affinity for DR4(III). DR4(I) is involved in rifampicin-mediated induction by PXR [32]. They suggest that DR4(II) does not contribute to the rifampicin-mediated induction by PXR even if the PXR/RXRα can bind DR4(II). In our study, PXR/RXRα formed a weak complex with DR4(II), and the −7833C>T substitution decreased the binding affinity of PXR/RXRα to DR4(II) (Fig. 1F). The −7833C>T substitution also decreased the transcriptional activation by PXR both in the presence and absence of rifampicin (Fig. 2F), but fold induction of MDR1 mRNA by rifampicin was not affected (Fig. 2E). These results suggest that DR4(II) does not contribute to rifampicin-activated MDR1 mRNA induction by PXR, which was consistent with previous observations [32]. PXR-dependent *MDR1* gene transcription without rifampicin was observed not only in this study, but also in other reports [32,43,44], and PXR-dependent CYP3A4 gene transcription without rifampicin also has been reported [32,43,44]. Since the −7833C>T substitution decreased PXR-dependent basal activation without rifampicin (Fig. 2F), DR4(II), which contains −7833C>T, may be involved in PXR-dependent basal MDR1 expression, not ligand-dependent expression. Although −7833C>T affected nuclear receptor (VDR, TRβ, CAR, and PXR)-mediated *MDR1* gene transactivation, it suppressed only about one third of total transactivity in each nuclear receptor (Fig. 2). We propose that this partial inhibition may be due to the multiple responsive elements that mediate MDR1 mRNA induction. Since xenobiotics and endogenous substrates-activated P-gp inductions play key roles in physiological functions [1,4,11,45], nuclear receptors might stimulate *MDR1* transcription through the multiple responsive elements.

Since the T-to-C substitution at nucleotide −1211 forms an XRE-like sequence (Fig. 3A) and AhR-induced MDR1 expression shows interindividual variation in human hepatocytes [37,46], we hypothesized that the −1211T>C substitution could affect the interindividual variation in MDR1 mRNA expression. However, AhR-dependent *MDR1* activation was not observed with either −1211T or −1211C (Fig. 3B), indicating that the −1211T>C substitution does not form a functional XRE. The −1211T>C substitution also forms an HRE-like sequence (Fig. 3A), and the −129T>C substitution, which is completely linkage disequilibrated with −1211T>C in Japanese [27,31], reportedly affects the expression level of MDR1 mRNA in intestine and colon cancer cells. Since the concentrations of oxygen in the intestine and cancer cells are relatively low compared to other tissues [30], it is possible that the −1211T>C substitution affects the HIF-induced MDR1 expression in a synergistic or inhibitory manner. However, the −1211T>C substitution could not affect the MDR1 expression, which was induced by a chemically-induced hypoxic condition, indicating that the −1211T>C substitution could not form the functional HRE (Fig. 3C).

In summary, we have demonstrated that the −7833C>T substitution in the *MDR1* gene decreases the binding affinities of nuclear receptors, VDR/RXRα, TRβ/RXRα, CAR, CAR/RXRα, and PXR/RXRα, to their responsive elements located around −7833. We also showed that the C-to-T substitution at −7833 reduces transcriptional activation of *MDR1* by VDR, TRβ, CAR, and PXR. However, another SNP at −1211 (T>C), which forms XRE-like and HRE-like sequences, failed to affect the AhR-dependent and hypoxia-induced *MDR1* transcriptional activation. Although the frequency of −7833C>T substitution in the *MDR1* gene is relatively low, knowledge of the −7833C>T substitution in *MDR1* is crucial for subjects who hold the −7833T allele because the pharmacokinetics of P-gp substrates may differ from wild-type profile. Further study, especially clinical studies, is necessary to confirm the functional significance of the −7833C>T substitution in the interindividual differences in P-gp expression level.

Acknowledgments

We thank Prof. Shuichi Koizumi (Yamanashi University, Japan) and Dr. Hideo Jinno (National Institute of Health Sciences, Japan) for providing the human RXRα cDNA and human CAR cDNA, respectively. This work was supported in part by grants from the Ministry of Health, Labor and Welfare of Japan (to M.T.) and the Japan Health Sciences Foundation (Research on Publicly Essential Drugs and Medical Devices) (to K.K.).

References

[1] V.J. Wacher, J.A. Silverman, Y. Zhang, L.Z. Benet, Role of P-glycoprotein and cytochrome P450 3A in limiting oral absorption of peptides and peptidomimetics, J. Pharm. Sci. 87 (1998) 1322–1330.
[2] T. Sakaeda, T. Nakamura, K. Okumura, MDR1 genotype-related pharmacokinetics and pharmacodynamics, Biol. Pharm. Bull. 25 (2002) 1391–1400.
[3] F. Thiebaut, T. Tsuruo, H. Hamada, M.M. Gottesman, I. Pastan, M.C. Willingham, Cellular localization of the multidrug-resistance gene product P-glycoprotein in normal human tissues, Proc. Natl Acad. Sci. USA 84 (1987) 7735–7738.
[4] M. Thorn, N. Finnstrom, S. Lundgren, A. Rane, L. Loof, Cytochromes P450 and MDR1 mRNA expression along the human gastrointestinal tract, Br. J. Clin. Pharmacol. 60 (2005) 54–60.
[5] C. Cordon-Cardo, J.P. O'Brien, D. Casals, L. Rittman-Grauer, J.L. Biedler, M.R. Melamed, J.R. Bertino, Multidrug-resistance gene (P-glycoprotein) is expressed by endothelial cells at blood–brain barrier sites, Proc. Natl Acad. Sci. USA 86 (1989) 695–698.
[6] P.B. Watkins, The barrier function of CYP3A4 and P-glycoprotein in the small bowel, Adv. Drug Deliv. Rev. 27 (1997) 161–170.
[7] J. Taipalensuu, H. Tornblom, G. Lindberg, C. Einarsson, F. Sjoqvist, H. Melhus, P. Garberg, B. Sjostrom, B. Lundgren, P. Artursson, Correlation of gene expression of ten drug efflux proteins of the ATP-binding cassette transporter family in normal human jejunum and in human intestinal epithelial Caco-2 cell monolayers, J. Pharmacol. Exp. Ther. 299 (2001) 164–170.
[8] C. Zimmermann, H. Gutmann, P. Hruz, J.P. Gutzwiller, C. Beglinger, J. Drewe, Mapping of multidrug resistance gene 1 and multidrug resistance-associated protein isoform 1 to 5 mRNA expression along the human intestinal tract, Drug Metab. Dispos. 33 (2005) 219–224.
[9] K. Sai, N. Kaniwa, M. Itoda, Y. Saito, R. Hasegawa, K. Komamura, K. Ueno, S. Kamakura, M. Kitakaze, K. Shirao, H. Minami, A. Ohtsu, T. Yoshida, N. Saijo, Y. Kitamura, N. Kamatani, S. Ozawa, J. Sawada, Haplotype analysis of ABCB1/MDR1 blocks in a Japanese population reveals genotype-dependent renal clearance of irinotecan, Pharmacogenetics 13 (2003) 741–757.
[10] K.N. Faber, M. Muller, P.L. Jansen, Drug transport proteins in the liver, Adv. Drug Deliv. Rev. 55 (2003) 107–124.
[11] A. Doran, R.S. Obach, B.J. Smith, N.A. Hosea, S. Becker, E. Callegari, C. Chen, X. Chen, E. Choo, J. Cianfrogna, L.M. Cox, J.P. Gibbs, M.A. Gibbs, H. Hatch, C.E. Hop, I.N. Kasman, J. Laperle, J. Liu, X. Liu, M. Logman, D. Maclin, F.M. Nedza, F. Nelson, E. Olson, S. Rahematpura, D. Raunig, S. Rogers, K. Schmidt, D.K. Spracklin, M. Szewc, M. Troutman, E. Tseng, M. Tu, J.W. Van Deusen, K. Venkatakrishnan, G. Walens, E.Q. Wang, D. Wong, A.S. Yasgar, C. Zhang, The impact of P-glycoprotein on the disposition of drugs targeted for indications of the central nervous system: evaluation using the MDR1A/1B knockout mouse model, Drug Metab. Dispos. 33 (2005) 165–174.
[12] N.H. Hendrikse, A.H. Schinkel, E.G. de Vries, E. Fluks, W.T. Van der Graaf, A.T. Willemsen, W. Vaalburg, E.J. Franssen, Complete in vivo reversal of P-glycoprotein pump function in the blood–brain barrier visualized with positron emission tomography, Br. J. Pharmacol. 124 (1998) 1413–1418.
[13] M.B. Muller, M.E. Keck, E.B. Binder, A.E. Kresse, T.P. Hagemeyer, R. Landgraf, F. Holsboer, M. Uhr, ABCB1 (MDR1)-type P-glycoproteins at the blood–brain barrier modulate the activity of the hypothalamic-pituitary-adrenocortical system: implications for affective disorder, Neuropsychopharmacology 28 (2003) 1991–1999.

[14] E.G. Schuetz, K.N. Furuya, J.D. Schuetz, Interindividual variation in expression of P-glycoprotein in normal human liver and secondary hepatic neoplasms, J. Pharmacol. Exp. Ther. 275 (1995) 1011–1018.
[15] K.S. Lown, R.R. Mayo, A.B. Leichtman, H.L. Hsiao, D.K. Turgeon, P. Schmiedlin-Ren, M.B. Brown, W. Guo, S.J. Rossi, L.Z. Benet, P.B. Watkins, Role of intestinal P-glycoprotein (mdr1) in interpatient variation in the oral bioavailability of cyclosporine, Clin. Pharmacol. Ther. 62 (1997) 248–260.
[16] A. Asghar, J.C. Gorski, B. Haehner-Daniels, S.D. Hall, Induction of multidrug resistance-1 and cytochrome P450 mRNAs in human mononuclear cells by rifampin, Drug Metab. Dispos. 30 (2002) 20–26.
[17] S. Taniguchi, Y. Mochida, T. Uchiumi, T. Tahira, K. Hayashi, K. Takagi, M. Shimada, Y. Maehara, H. Kuwano, S. Kono, H. Nakano, M. Kuwano, M. Wada, Genetic polymorphism at the 5′ regulatory region of multidrug resistance 1 (MDR1) and its association with interindividual variation of expression level in the colon, Mol. Cancer Ther. 2 (2003) 1351–1359.
[18] R. Kerb, A.S. Aynacioglu, J. Brockmoller, R. Schlagenhaufer, S. Bauer, T. Szekeres, A. Hamwi, M. Fritzer-Szekeres, C. Baumgartner, H.Z. Ongen, P. Guzelbey, I. Roots, U. Brinkmann, The predictive value of MDR1, CYP2C9, and CYP2C19 polymorphisms for phenytoin plasma levels, Pharmacogenomics J. 1 (2001) 204–210.
[19] U. Brinkmann, M. Eichelbaum, Polymorphisms in the ABC drug transporter gene MDR1, Pharmacogenomics J. 1 (2001) 59–64.
[20] S. Saito, A. Iida, A. Sekine, Y. Miura, C. Ogawa, S. Kawauchi, S. Higuchi, Y. Nakamura, Three hundred twenty-six genetic variations in genes encoding nine members of ATP-binding cassette, subfamily B (ABCB/MDR/TAP), in the Japanese population, J. Hum. Genet. 47 (2002) 38–50.
[21] R.B. Kim, B.F. Leake, E.F. Choo, G.K. Dresser, S.V. Kubba, U.I. Schwarz, A. Taylor, H.G. Xie, J. McKinsey, S. Zhou, L.B. Lan, J.D. Schuetz, E.G. Schuetz, G.R. Wilkinson, Identification of functionally variant MDR1 alleles among European Americans and African Americans, Clin. Pharmacol. Ther. 70 (2001) 189–199.
[22] C. Kimchi-Sarfaty, J.M. Oh, I.W. Kim, Z.E. Sauna, A.M. Calcagno, S.V. Ambudkar, M.M. Gottesman, A "silent" polymorphism in the MDR1 gene changes substrate specificity, Science 315 (2007) 525–528.
[23] S. Hoffmeyer, O. Burk, O. von Richter, H.P. Arnold, J. Brockmoller, A. Johne, I. Cascorbi, T. Gerloff, I. Roots, M. Eichelbaum, U. Brinkmann, Functional polymorphisms of the human multidrug-resistance gene: multiple sequence variations and correlation of one allele with P-glycoprotein expression and activity in vivo, Proc. Natl Acad. Sci. USA 97 (2000) 3473–3478.
[24] D. Wang, A.D. Johnson, A.C. Papp, D.L. Kroetz, W. Sadee, Multidrug resistance polypeptide 1 (MDR1, ABCB1) variant 3435C>T affects mRNA stability, Pharmacogenet. Genomics 15 (2005) 693–704.
[25] T. Sakaeda, T. Nakamura, M. Horinouchi, M. Kakumoto, N. Ohmoto, T. Sakai, Y. Morita, T. Tamura, N. Aoyama, M. Hirai, M. Kasuga, K. Okumura, MDR1 genotype-related pharmacokinetics of digoxin after single oral administration in healthy Japanese subjects, Pharm. Res. 18 (2001) 1400–1404.
[26] N. Morita, T. Yasumori, K. Nakayama, Human MDR1 polymorphism: G2677T/A and C3435T have no effect on MDR1 transport activities, Biochem. Pharmacol. 65 (2003) 1843–1852.
[27] Y. Moriya, T. Nakamura, M. Horinouchi, T. Sakaeda, T. Tamura, N. Aoyama, T. Shirakawa, A. Gotoh, S. Fujimoto, M. Matsuo, M. Kasuga, K. Okumura, Effects of polymorphisms of MDR1, MRP1, and MRP2 genes on their mRNA expression levels in duodenal enterocytes of healthy Japanese subjects, Biol. Pharm. Bull. 25 (2002) 1356–1359.
[28] B. Wang, S. Ngoi, J. Wang, S.S. Chong, C.G. Lee, The promoter region of the MDR1 gene is largely invariant, but different single nucleotide polymorphism haplotypes affect MDR1 promoter activity differently in different cell lines, Mol. Pharmacol. 70 (2006) 267–276.
[29] H. Takane, D. Kobayashi, T. Hirota, J. Kigawa, N. Terakawa, K. Otsubo, I. Ieiri, Haplotype-oriented genetic analysis and functional assessment of promoter variants in the MDR1 (ABCB1) gene, J. Pharmacol. Exp. Ther. 311 (2004) 1179–1187.
[30] T. Koyama, T. Nakamura, C. Komoto, T. Sakaeda, M. Taniguchi, N. Okamura, T. Tamura, N. Aoyama, T. Kamigaki, Y. Kuroda, M. Kasuga, K. Kadoyama, K. Okumura, MDR1 T-129C polymorphism can be predictive of differentiation, and thereby prognosis of colorectal adenocarcinomas in Japanese, Biol. Pharm. Bull. 29 (2006) 1449–1453.
[31] W. Qian, M. Homma, F. Itagaki, H. Tachikawa, Y. Kawanishi, K. Mizukami, T. Asada, S. Inomata, K. Honda, N. Ohkohchi, Y. Kohda, MDR1 gene polymorphism in Japanese patients with schizophrenia and mood disorders including depression, Biol. Pharm. Bull. 29 (2006) 2446–2450.
[32] A. Geick, M. Eichelbaum, O. Burk, Nuclear receptor response elements mediate induction of intestinal MDR1 by rifampin, J. Biol. Chem. 276 (2001) 14581–14587.
[33] O. Burk, K.A. Arnold, A. Geick, H. Tegude, M. Eichelbaum, A role for constitutive androstane receptor in the regulation of human intestinal MDR1 expression, Biol. Chem. 386 (2005) 503–513.
[34] K. Kurose, M. Saeki, M. Tohkin, R. Hasegawa, Thyroid hormone receptor mediates human MDR1 gene expression—identification of the response region essential for gene expression, Arch. Biochem. Biophys. 474 (2008) 82–90.
[35] M. Saeki, K. Kurose, M. Tohkin, R. Hasegawa, Identification of the functional vitamin D response elements in the human MDR1 gene, Biochem. Pharmacol. 76 (2008) 531–542.
[36] K. Sai, M. Itoda, Y. Saito, K. Kurose, N. Katori, N. Kaniwa, K. Komamura, T. Kotake, H. Morishita, H. Tomoike, S. Kamakura, M. Kitakaze, T. Tamura, N. Yamamoto, H. Kunitoh, Y. Yamada, Y. Ohe, Y. Shimada, K. Shirao, H. Minami, A. Ohtsu, T. Yoshida, N. Saijo, N. Kamatani, S. Ozawa, J. Sawada, Genetic variations and haplotype structures of the ABCB1 gene in a Japanese population: an expanded haplotype block covering the distal promoter region, and associated ethnic differences, Ann. Hum. Genet. 70 (2006) 605–622.
[37] E. Jigorel, M. Le Vee, C. Boursier-Neyret, Y. Parmentier, O. Fardel, Differential regulation of sinusoidal and canalicular hepatic drug transporter expression by xenobiotics activating drug-sensing receptors in primary human hepatocytes, Drug Metab. Dispos. 34 (2006) 1756–1763.
[38] K.M. Comerford, T.J. Wallace, J. Karhausen, N.A. Louis, M.C. Montalto, S.P. Colgan, Hypoxia-inducible factor-1-dependent regulation of the multidrug resistance (MDR1) gene, Cancer Res. 62 (2002) 3387–3394.
[39] S. Koyano, Y. Saito, H. Fukushima-Uesaka, S. Ishida, S. Ozawa, N. Kamatani, H. Minami, A. Ohtsu, T. Hamaguchi, K. Shirao, T. Yoshida, N. Saijo, H. Jinno, J. Sawada, Functional analysis of six human aryl hydrocarbon receptor variants in a Japanese population, Drug Metab. Dispos. 33 (2005) 1254–1260.
[40] H. Jinno, T. Tanaka-Kagawa, N. Hanioka, S. Ishida, M. Saeki, A. Soyama, M. Itoda, T. Nishimura, Y. Saito, S. Ozawa, M. Ando, J. Sawada, Identification of novel alternative splice variants of human constitutive androstane receptor and characterization of their expression in the liver, Mol. Pharmacol. 65 (2004) 496–502.
[41] K. Kurose, M. Tohkin, M. Fukuhara, A novel positive regulatory element that enhances hamster CYP2A8 gene expression mediated by xenobiotic responsive element, Mol. Pharmacol. 55 (1999) 279–287.
[42] J.M. Gow, L.W. Chinn, D.L. Kroetz, The effects of ABCB1 3′-untranslated region variants on mRNA stability, Drug Metab. Dispos. 36 (2008) 10–15.
[43] A. Pfrunder, H. Gutmann, C. Beglinger, J. Drewe, Gene expression of CYP3A4, ABC-transporters (MDR1 and MRP1-MRP5) and hPXR in three different human colon carcinoma cell lines, J. Pharm. Pharmacol. 55 (2003) 59–66.
[44] L. Cerveny, L. Svecova, E. Anzenbacherova, R. Vrzal, F. Staud, Z. Dvorak, J. Ulrichova, P. Anzenbacher, P. Pavek, Valproic acid induces CYP3A4 and MDR1 gene expression by activation of constitutive androstane receptor and pregnane X receptor pathways, Drug Metab. Dispos. 35 (2007) 1032–1041.
[45] S. Marchetti, R. Mazzanti, J.H. Beijnen, J.H. Schellens, Concise review: clinical relevance of drug–drug and herb–drug interactions mediated by the ABC transporter ABCB1 (MDR1, P-glycoprotein), Oncologist 12 (2007) 927–941.
[46] P. Olinga, M.G. Elferink, A.L. Draaisma, M.T. Merema, J.V. Castell, G. Perez, G.M. Groothuis, Coordinated induction of drug transporters and phase I and II metabolism in human liver slices, Eur. J. Pharm. Sci. 33 (2008) 380–389.

The Pharmacogenomics Journal (2011), 1–10

www.nature.com/tpj

ORIGINAL ARTICLE

A whole-genome association study of major determinants for allopurinol-related Stevens–Johnson syndrome and toxic epidermal necrolysis in Japanese patients

M Tohkin[1,8], N Kaniwa[1,8], Y Saito[1,8], E Sugiyama[1,8], K Kurose[1,8], J Nishikawa[1,8], R Hasegawa[1,8], M Aihara[2,8], K Matsunaga[3,8], M Abe[3,8], H Furuya[4,8], Y Takahashi[5,8], H Ikeda[5,8], M Muramatsu[6,8], M Ueta[7,8], C Sotozono[7,8], S Kinoshita[7,8], Z Ikezawa[2,8] and the Japan Pharmacogenomics Data Science Consortium[9]

[1]*Department of Medicinal Safety Science, National Institute of Health Sciences, Tokyo, Japan;* [2]*Department of Environmental Immunodermatology, Yokohama City University Graduate School of Medicine, Yokohama, Japan;* [3]*Department of Dermatology, Fujita Health University School of Medicine, Toyoake, Japan;* [4]*Department of Neurology, Neuro-Muscular Center, National Oomuta Hospital, Oomuta, Japan;* [5]*Shizuoka Institute of Epilepsy and Neurological Disorders, National Epilepsy Center, Shizuoka, Japan;* [6]*Department of Molecular Epidemiology, Medical Research Institute, Tokyo Medical and Dental University, Tokyo, Japan and* [7]*Department of Ophthalmology, Kyoto Prefectural University of Medicine, Kyoto, Japan*

Correspondence:
Dr M Tohkin, Department of Medicinal Safety Science, Graduate School of Pharmaceutical Sciences, Nagoya City University, 3-1 Tanabe-dori, Mizuho-ku, Nagoya 467-8603, Japan.
E-mail: tohkin@phar.nagoya-cu.ac.jp

[8]Members of the Japan Severe Adverse Reaction (JSAR) research group.
[9]The members of the Japan Pharmacogenomics Data Science Consortium are listed in the Appendix.

Received 12 January 2011; revised 10 August 2011; accepted 11 August 2011

Stevens–Johnson syndrome and toxic epidermal necrolysis (SJS/TEN) are severe, cutaneous adverse drug reactions that are rare but life threatening. Genetic biomarkers for allopurinol-related SJS/TEN in Japanese were examined in a genome-wide association study in which Japanese patients ($n=14$) were compared with ethnically matched healthy controls ($n=991$). Associations between 890 321 single nucleotide polymorphisms and allopurinol-related SJS/TEN were analyzed by the Fisher's exact test (dominant genotype mode). A total of 21 polymorphisms on chromosome 6 were significantly associated with allopurinol-related SJS/TEN. The strongest association was found at rs2734583 in *BAT1*, rs3094011 in *HCP5* and GA005234 in *MICC* ($P=2.44\times10^{-8}$; odds ratio = 66.8; 95% confidence interval, 19.8–225.0). rs9263726 in *PSORS1C1*, also significantly associated with allopurinol-related SJS/TEN, is in absolute linkage disequilibrium with *human leukocyte antigen-B*5801*, which is in strong association with allopurinol-induced SJS/TEN. The ease of typing rs9263726 makes it a useful biomarker for allopurinol-related SJS/TEN in Japanese.
The Pharmacogenomics Journal advance online publication, 13 September 2011; doi:10.1038/tpj.2011.41

Keywords: allopurinol; Stevens–Johnson syndrome; toxic epidermal necrolysis; human lymphocyte antigen; single nucleotide polymorphism; genome-wide association study

Introduction

Allopurinol is a xanthine oxidase inhibitor that prevents the production of uric acid to reduce plasma uric acid levels to a normal range. It is the most frequently used anti-hyperuricemic agent in the world due to its long-term pharmacological effect.[1] However, allopurinol is also one of the most frequent causes of a variety of delayed severe cutaneous adverse drug reactions (SCARs).[2] According to spontaneous reports of severe adverse drug reactions to the Ministry of Health, Labor, and Welfare of Japan, allopurinol-related SCARs accounted for about 11% of all reported SCAR cases in Japan in 2008.[3] Allopurinol-related SCARs include the drug-induced hypersensitivity syndrome, Stevens–Johnson syndrome (SJS) and toxic epidermal necrolysis (TEN).[4] SJS/TEN are characterized by high fever, malaise and rapid development of blistering exanthema, with macules and target-like lesions, accompanied by mucosal involvement.[5] Even though the incidence of SJS/TEN is extremely low, the mortality rate of TEN can be as high as 26%.[5] Therefore, SJS/TEN is a serious problem in allopurinol therapy, in spite of the ideal anti-hyperuricemic effect of allopurinol.

Although previous works have suggested that the development of SJS/TEN depends on an immune mechanism involving a drug-dependent cytotoxic cell response against epidermal cells,[5,6] the pathophysiology of SJS/TEN remains largely unknown. Susceptibility to such idiosyncratic reactions is thought to be genetically determined, and familial predisposition to allopurinol-induced SJS/TEN has been reported.[6] Therefore, the exploratory studies for genetic risk factors related to SJS/TEN are needed. A strong association has been observed between allopurinol-induced SCAR and the human lymphocyte antigen (*HLA*) allele B variant (*HLA-B*5801*) in the Han Chinese in Taiwan[7] and in the Thai population.[8] These studies showed that the *HLA-B*5801* allele is present in all patients with allopurinol-induced SCAR (51/51 of Han Chinese and 27/27 of Thai patients) and in only 12–15% of tolerant patients (20/135 and 7/54, respectively). The odds ratio (OR) was 580 (95% confidence interval , 34–9781; $P=4.7\times10^{24}$) for the Han-Chinese data[7] and 348.3 (95% confidence interval, 19.2–6336.9; $P=1.61\times10^{13}$) for the Thai study.[8] Although the association was confirmed in both Caucasian and Japanese subjects,[9,10] the OR in the Han-Chinese and Thai populations were much higher than those in the Caucasian (OR = 80) and Japanese (OR = 40) groups. These reports indicated that *HLA-B*5801* is the valid genetic biomarker for allopurinol-induced SJS/TEN in various ethnic groups, but the mechanisms by which *HLA-B*5801* is specifically involved in allopurinol-induced SJS/TEN progression and the strength of the association showed ethnic differences are unknown.

Currently, genotyping by high-density array scanning of the whole genome allows discovery of previously unsuspected genetic risk factors that influence the pathogenesis of serious adverse drug reactions.[11–13] Genome-wide association studies (GWASs) provide opportunities to uncover polymorphisms that influence susceptibility to allopurinol-induced SJS/TEN free of mechanistic hypotheses. Therefore, in addition to *HLA-B* typing as shown in our previous study,[10] we further conducted a retrospective pharmacogenetic case–control study using whole-genome single nucleotide polymorphism (SNP) data from high-density DNA microarrays in order to identify new and effective genetic biomarkers for allopurinol-related SJS/TEN in Japanese patients.

Materials and methods

Recruitment of study subjects

A total of 141 Japanese SJS/TEN patients from unrelated families were recruited from July 2006 to April 2010 from participating institutes of the Japan Severe Adverse Reactions (JSAR) research group and through a nationwide blood-sampling network system in Japan for SJS/TEN onset patients, operated by the National Institute of Health Sciences.[10] In all, 121 of these patients were diagnosed as defined SJS or TEN by JSAR research group's dermatological experts based on diagnostic criteria[4] that are currently used in Japan. Information was collected using a standardized case report form that includes medical records, co-administrated drug records, disease progress and involvement of systemic complications, as well as SJS/TEN treatment. Among the 141 SJS/TEN patients, 20 were diagnosed as probable SJS due to atypical or mild symptoms. TEN and SJS were defined as mucocutaneous disorders characterized by extensive erythema, blisters, epidermal detachment, erosions, enanthema and high fever. SJS was defined as skin detachment of 10% or less of the body surface area, and TEN as skin detachment of more than 10%, excluding staphylococcal scaled skin syndrome.[5] In all enrolled cases defined as SJS or TEN, allopurinol was regarded as the drug responsible for SJS or TEN if the onset of SJS/TEN symptoms occurred within the first 2 months of allopurinol exposure. For the retrospective pharmacogenetic case–control study, 991 healthy, ethnically matched subjects in the Tokyo metropolitan area were used as the control group. Healthy subjects were used as the control group instead of allopurinol-tolerant patients because the incidence of SJS/TEN is extremely low (0.4–6 per million per year).[3]

The ethics committees of the National Institute of Health Sciences, each participating institute of the JSAR research group and the Japan Pharmacogenomics Data Science Consortium (JPDSC) approved this study. Written informed consent was obtained from all cases and ethnically matched controls.

Whole-genome genotyping of SNPs

Genome-wide genotyping of the 14 allopurinol-related SJS/TEN patients and 991 ethnically matched controls was conducted using the Illumina Human 1M-Duo BeadChip (Illumina, San Diego, CA, USA), which contained 11 63 218 SNPs. SNPs were discarded from case–control association analysis if they exhibited a minor allele frequency <0.001 in the control group (2 37 890 SNPs), a call rate <0.95 for each SNP (32 640 SNPs) or a *P*-value <0.001 in the test of Hardy–Weinberg equilibrium among controls (2 368 SNPs). These quality control steps removed a total of 2 72 897 SNPs. All samples had a call rate for each microarray above 0.99. Sample duplicates and hidden relatedness were investigated on the basis of pairwise identity-by-state analysis via PLINK;[14] however, there was no duplicate or hidden relatedness in the samples. This quality-control procedure ensured reliable genotyping data.

HLA genotyping and TaqMan genotyping of SNPs on chromosome 6

HLA A, *B* and *Cw* types were determined using sequencing-based methods, as described previously.[10] Representative SNPs of 6p21 (rs2734583, rs3099844, rs9263726 and rs3131643) were re-genotyped using TaqMan SNP Genotyping Assays (Life Technologies, Carlsbad, CA, USA) (ID; C__27465749_10, C__27455402_10, C__30352071_10, C__26778946_20) according to the manufacturer's instruction using 5 ng of genomic DNA. We did not genotype rs9267445 and rs1634776 because TaqMan SNP genotyping assays for these SNPs were not available. Measurement of the linkage disequilibrium (LD) coefficient was performed using